

AWARD NUMBER: W81XWH-13-1-0138

TITLE: In Vivo 18-FDG/18-Choline-Mediated Cerenkov Radiation Energy Transfer (CRET) Multiplexed Optical Imaging for Human Prostate Carcinoma Detection and Staging

PRINCIPAL INVESTIGATOR: Susan L. Deutscher, Ph.D.

CONTRACTING ORGANIZATION: University of Missouri System
Columbia MO 65211-3020

REPORT DATE: December 2017

TYPE OF REPORT: Final

PREPARED FOR: U.S. Army Medical Research and Materiel Command
Fort Detrick, Maryland 21702-5012

DISTRIBUTION STATEMENT: Approved for Public Release;
Distribution Unlimited

The views, opinions and/or findings contained in this report are those of the author(s) and should not be construed as an official Department of the Army position, policy or decision unless so designated by other documentation.

REPORT DOCUMENTATION PAGE

Form Approved
OMB No. 0704-0188

Public reporting burden for this collection of information is estimated to average 1 hour per response, including the time for reviewing instructions, searching existing data sources, gathering and maintaining the data needed, and completing and reviewing this collection of information. Send comments regarding this burden estimate or any other aspect of this collection of information, including suggestions for reducing this burden to Department of Defense, Washington Headquarters Services, Directorate for Information Operations and Reports (0704-0188), 1215 Jefferson Davis Highway, Suite 1204, Arlington, VA 22202-4302. Respondents should be aware that notwithstanding any other provision of law, no person shall be subject to any penalty for failing to comply with a collection of information if it does not display a currently valid OMB control number. **PLEASE DO NOT RETURN YOUR FORM TO THE ABOVE ADDRESS.**

1. REPORT DATE December 2017		2. REPORT TYPE Final		3. DATES COVERED 16 Sept 2013 - 15 Sept 2017	
4. TITLE AND SUBTITLE In Vivo 18-FDG/18-Choline-Mediated Cerenkov Radiation Energy Transfer (CRET) Multiplexed Optical Imaging for Human Prostate Carcinoma Detection and Staging				5a. CONTRACT NUMBER	
				5b. GRANT NUMBER W81XWH-13-1-0138	
				5c. PROGRAM ELEMENT NUMBER	
6. AUTHOR(S) Susan L. Deutscher, Ph.D. E-Mail: E-Mail:deutschers@missouri.edu				5d. PROJECT NUMBER	
				5e. TASK NUMBER	
				5f. WORK UNIT NUMBER	
7. PERFORMING ORGANIZATION NAME(S) AND ADDRESS(ES) University of Missouri System 316 University Hall Columbia MO 65211-3020				8. PERFORMING ORGANIZATION REPORT NUMBER	
9. SPONSORING / MONITORING AGENCY NAME(S) AND ADDRESS(ES) U.S. Army Medical Research and Materiel Command Fort Detrick, Maryland 21702-5012				10. SPONSOR/MONITOR'S ACRONYM(S)	
				11. SPONSOR/MONITOR'S REPORT NUMBER(S)	
12. DISTRIBUTION / AVAILABILITY STATEMENT Approved for Public Release; Distribution Unlimited					
13. SUPPLEMENTARY NOTES					
14. ABSTRACT Prostate cancer is treatable in its earliest stages, although treatment options for advanced forms are limited. Therefore, more sensitive means of early prostate cancer detection and new prostate cancer therapies are needed. Two novel biomarkers are proposed to associate with prostate cancer progression: the Thomsen-Friedenreich disaccharide (TF) antigen and the ErbB-2/ErbB-3 heterodimer (ErbB2/3). The objective of this proposal is to examine whether internal illumination via 18Ffluorocholine/18F-FDG Cerenkov radiation energy transfer (CRET) coupled with TF- and ErbB2/3- molecularly targeted nearinfrared (NIR) QDs can be used to detect prostate cancer. We have shown that ErbB2/ErbB3 dimerization is heregulin mediated and upregulated in castrated mice bearing MDA-PCa-2b human prostate cancer xenografts. We have selected peptides from bacteriophage display libraries that target TF and ErbB2/ErbB3. The peptides have been attached to QDs and have been used to detect human prostate cancer cell lines that express TF, ErbB2/ErbB3. Biodistribution studies were performed in MDA-PCa-2b human prostate cancer castrated and uncastrated mice. The anti-TF and anti-ErbB3 QD could be visualized in MDA-PCa2b human prostate cancer xenografts using an ex vivo-in vivo CRET imaging protocol.					
15. SUBJECT TERMS prostate cancer, ErbB2, ErbB3, molecular imaging, PET, phage display, TF antigen					
16. SECURITY CLASSIFICATION OF:			17. LIMITATION OF ABSTRACT	18. NUMBER OF PAGES	19a. NAME OF RESPONSIBLE PERSON
a. REPORT	b. ABSTRACT	c. THIS PAGE			USAMRMC
Unclassified	Unclassified	Unclassified	Unclassified	34	19b. TELEPHONE NUMBER (include area code)

Table of Contents

Introduction.....	4
Body.....	4
Key Research Accomplishments.....	31
Reportable Outcomes.....	31
Conclusions.....	31
References.....	32
Bibliography.....	32
Personnel.....	32
Appendices.....	32

Introduction

Prostate cancer is treatable in its earliest stages, although treatment options for advanced forms are limited. Therefore, more sensitive means of early prostate cancer detection and new prostate cancer therapies are needed. Unquestionably, better biomarkers of prostate cancer would assist in diagnosis, predicting disease course, and therapy. Two novel biomarkers are proposed to associate with prostate cancer progression: the Thomsen-Friedenreich disaccharide (TF) antigen and the ErbB-2/ErbB-3 heterodimer (ErbB2/3). TF is a pan-carcinoma antigen expressed on 90% of carcinomas, including early and late stage prostate carcinomas. The ErbB2/3 heterodimer is thought to occur in ~85% of prostate cancers and is a biomarker for progression, aggressiveness, and recurrence in castration resistant prostate cancer. These biomarkers may serve as a foundation for new prostate cancer diagnostic imaging and therapeutic agents. Both molecular and functional imaging have gained attention as potential cancer diagnostics. Quantum dots (QDs) are being employed for in vivo molecular imaging because of their broad spectrum excitation, high fluorescence quantum yields, and large effective Stokes shifts; however, they are not ideal for use in vivo due to external visible light requirements and the resulting autofluorescence. Functional imaging utilizing positron emission tomography (PET) is currently in the clinic, and uptake of the PET tracers ^{18}F -fluorodeoxyglucose (FDG) and ^{18}F -fluorocholine in prostate tumors has been demonstrated. Unfortunately, distinction between benign and cancerous tissues with these PET tracers is not possible. A solution to this problem would be to couple QD based molecular imaging with ^{18}F -fluorocholine (or ^{18}F -FDG) radiation-luminescence (i.e. Cerenkov radiation) resulting from the ^{18}F positron emission as an internal source of illumination. The objective of this proposal is to examine whether internal illumination via ^{18}F -fluorocholine Cerenkov radiation energy transfer (CRET) coupled with TF- and ErbB2/3- molecularly targeted near-infrared (NIR) QDs can be used to detect prostate cancer. ^{18}F -fluorocholine PET imaging will be utilized to define the metabolically active tumor tissue, while molecularly targeted QDs will facilitate biomarker-specific diagnosis.

The specific aims of the proposal are to: 1) select peptides that target the ErbB2/3 heterodimer using novel parallel in vitro/in vivo phage display techniques; 2) generate NIR-QDs decorated with TF- and ErbB2/3-avid peptides for in vivo molecular targeting; and 3) employ multimodal, multiplexed in vivo imaging of choline uptake, and ErbB2/3- and TF- expression in various stages of prostate cancer in mouse models of human cancer.

Keywords: Cerenkov radiation energy transfer (CRET), ErbB2, ErbB3, molecular imaging, PET, phage display, prostate cancer, quantum dots (QDs), Thomsen-Friedenreich disaccharide (TF).

Overall Project Summary

Task 1. Parallel In Vitro Phage Display Selection and In Vivo Phage Display Selection (months 1-10). Completed

a. Purify ErbB2 ECD and characterize purified ErbB2/ErbB3 ECD heterodimer in preparation for in vitro selections (month 1-2).

Progress: Human embryonic kidney (HEK) cells were transfected with ErbB2 expressing vector containing Flag epitope (plasmid c-erbB-2-pRc/ CMVFLAG) encoding ErbB-2-ECD tagged with a FLAG sequence for purification (1). Cells were grown in RPMI, gentamicin and G418 for selection. Cultured supernatant was sterile filtered through 0.22 μm filter and applied to an anti-FLAG affinity column equilibrated with 20 mM of Tris (pH 8.0) and 150 mM of NaCl. Bound protein was eluted with 0.1 M of glycine (pH 3.0) and neutralized with 1M of Tris HCl (pH 8.0). The protein was concentrated and dialyzed against PBS. So far, 25 mg of protein has been purified. The protein is stable in PBS in the refrigerator for at least one month and in PBS/40% glycerol for at least one year.

To facilitate dimerization, ErbB2 and ErbB3 with antibody Fc portions were utilized. Both purified ErbB2 and ErbB3 with Fc tags were purchased from Sino Inc. The proteins are stable for one year at -20°C.

A heterodimer of ErbB2 and ErbB3 was formed by treatment of ErbB2 with heregulin (HRG), addition of ErbB3 and dimer formation was observed and monitored by ELISA (Figure 1). As shown, the ErbB2 with the Fc tag formed much more heterodimer than flag tagged ErbB2. A complex of ErbB2 and ErbB3 without addition of HRG was also formed as confirmed by ELISA (Figure 2).

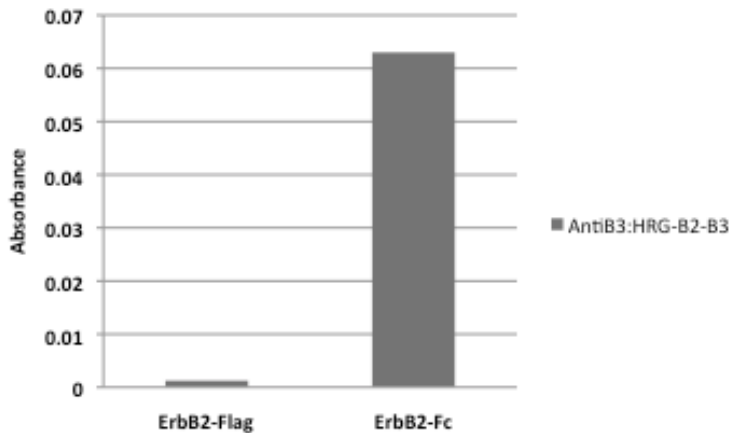


Figure 1. ErbB2/ErbB3 Heterodimer Formation. Anti- ErbB3 antibody was coated overnight on a 96 well plate. Wells were blocked 2/ErbB3 was captured in the wells. The plate was washed and incubated with Anti-ErbB2 antibody. Wells were washed and incubated with HRP conjugated secondary, washed again and the plate was developed. Absorbance was read, with background subtracted.

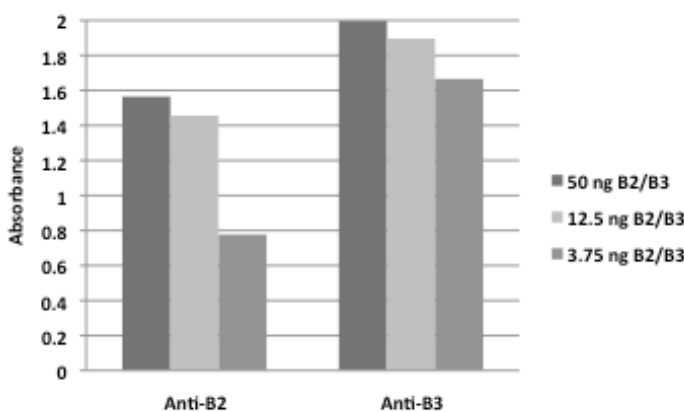


Figure 2. ErbB2/ErbB3 ELISA. ErbB2 and ErbB3 were incubated together in a 96 well plate, at various concentrations. Plates were blocked and incubated with either Anti-ErbB2 antibody or Anti-ErbB3 antibody. Wells were washed and incubated with appropriate HRP conjugated secondary, washed again and developed. Absorbance was read and background subtracted.

b. Inoculate sixteen mice with MDA-PCa-2b human prostate carcinoma cell line in preparation for in vivo selections (month 3).

Progress: Sixteen nude mice were inoculated with MDA-PCa-2b cells in two batches of eight mice. Approximately 75% of the mice grew tumors and in 20% of these, tumors would regress after one month. We are performing histopathology studies on large and small (regressed) tumors to grade tumors. The in vivo selections are being performed in mice with non-regressing tumors.

c. Perform parallel in vitro phage display selections against ErbB2 ECD, ErbB3 ECD, and ErbB2/ErbB3 ECD heterodimer (months 3-6).

Progress: The selections were performed as outlined in Figure 3 and Figure 4. Parallel ErbB2 and ErbB3 selections were also performed.

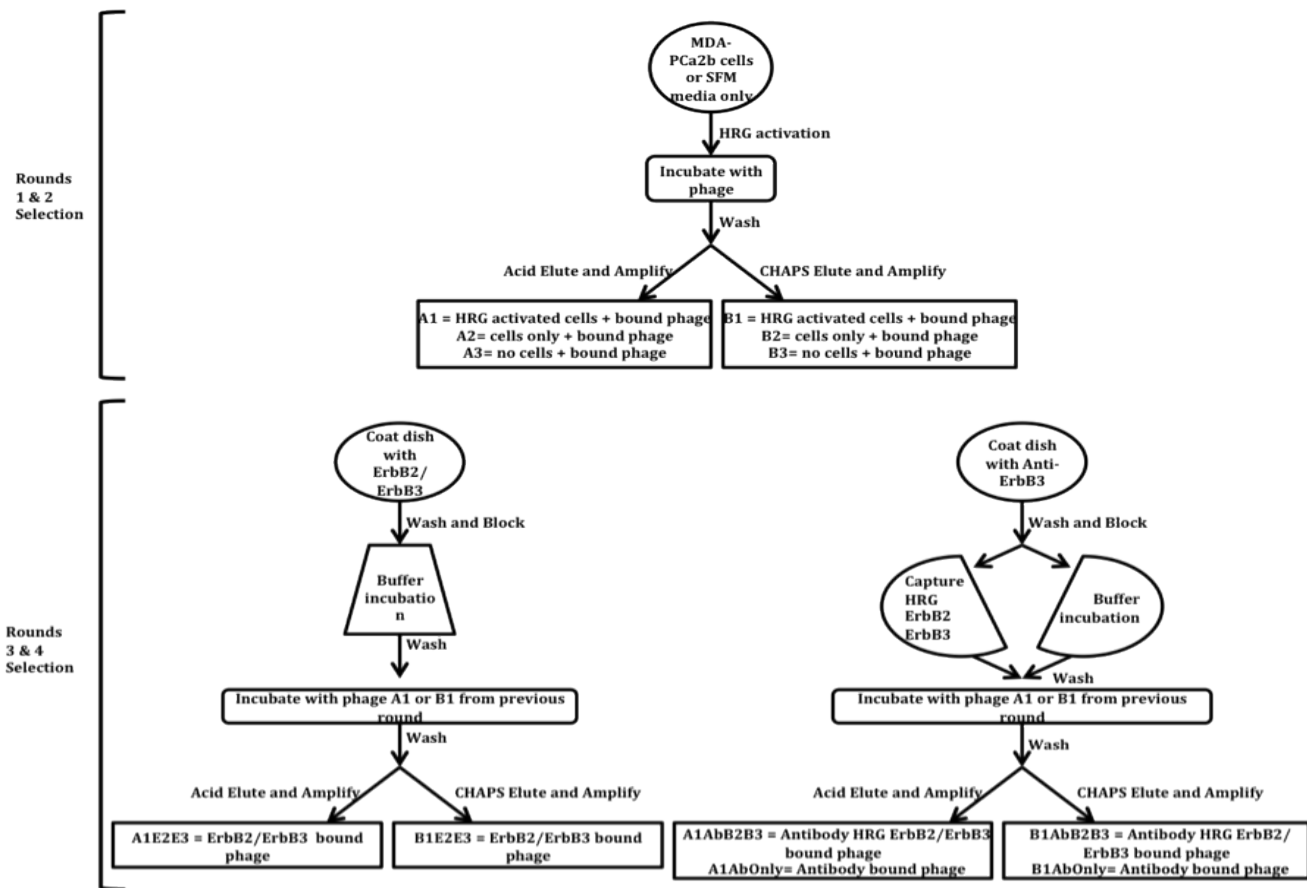


Figure 3. Selection Strategy Rounds 1-4. 1st and 2nd round selection: In a 6 well plate (Row A and Row B), MDA-PCa2b cells plated in first 2 wells each row and last well each row had media only. Twenty four hours before selection, replace growth media with serum free media (SFM) in all six wells. In first wells of each row add HRG 100ng/mL for 10 minutes at 37°C. Remove all media from wells and replace with SFM containing 1013V/mL. Incubate 30 minutes at 37°C. Wash 1X (round 2 wash 3X) and elute phage. Acid elute top row in 800µL 0.1 N HCl, pH 2.2 with glycine for 10 min and neutralize. CHAPS elute bottom row in 1mL 2.5% CHAPS for 10 min. keep each well eluate separate and amplify and purify phage, saving cell pellets for RF DNA extraction. Each subsequent round of selection will use the amplified, eluted phage from the previous round as input. 3rd and 4th round selection: Two parallel selections for each round. One uses ErbB2 and ErbB3 coated directly on the plate. The other selection uses antibody to capture the HRG/ErbB2/ErbB3. In a 96 well plate coat 6 wells with 50 µL ErbB2 + 50 µL ErbB3 (50ng R3 and 25ng R4) in Na Carb pH9 buffer and 12 wells with 100 µL anti ErbB3 antibody (1µg/mL) in Na Carb pH9 buffer, overnight at 4°C. Wash plate and block wells with 400µL 5%BSA in TBS, 2 hours at RT. Aspirate blocking buffer. Add 100µL TBS to 6 ErbB2/ErbB3 wells and 6 antibody wells. Add 100µL of HRGErbB2/ErbB3 mixture in TBS in 6 of the antibody wells (premixed 30 minutes in advance: 3µg/mL ErbB2, 1µg/mL ErbB3-ECD (Sino), 1µg/mL HRG) and incubate 30 min at RT. Wash plate and add 100µL of 1012 V/mL phage in TBS to the appropriate wells (A1 phage for acid elute wells and B1 phage for the CHAPS elute wells). Incubate at 4°C for 4 hours. Wash plate (2X Round 3 and 4X Round 4) and elute bound phage. Acid elute appropriate wells in 200µL 0.1 N HCl, pH 2.2 with glycine for 10 min and neutralize. CHAPS elute appropriate wells in 200uL 2.5% CHAPS for 10 min. Amplify and purify phage as input for next round, saving cell pellets for RF DNA extraction.

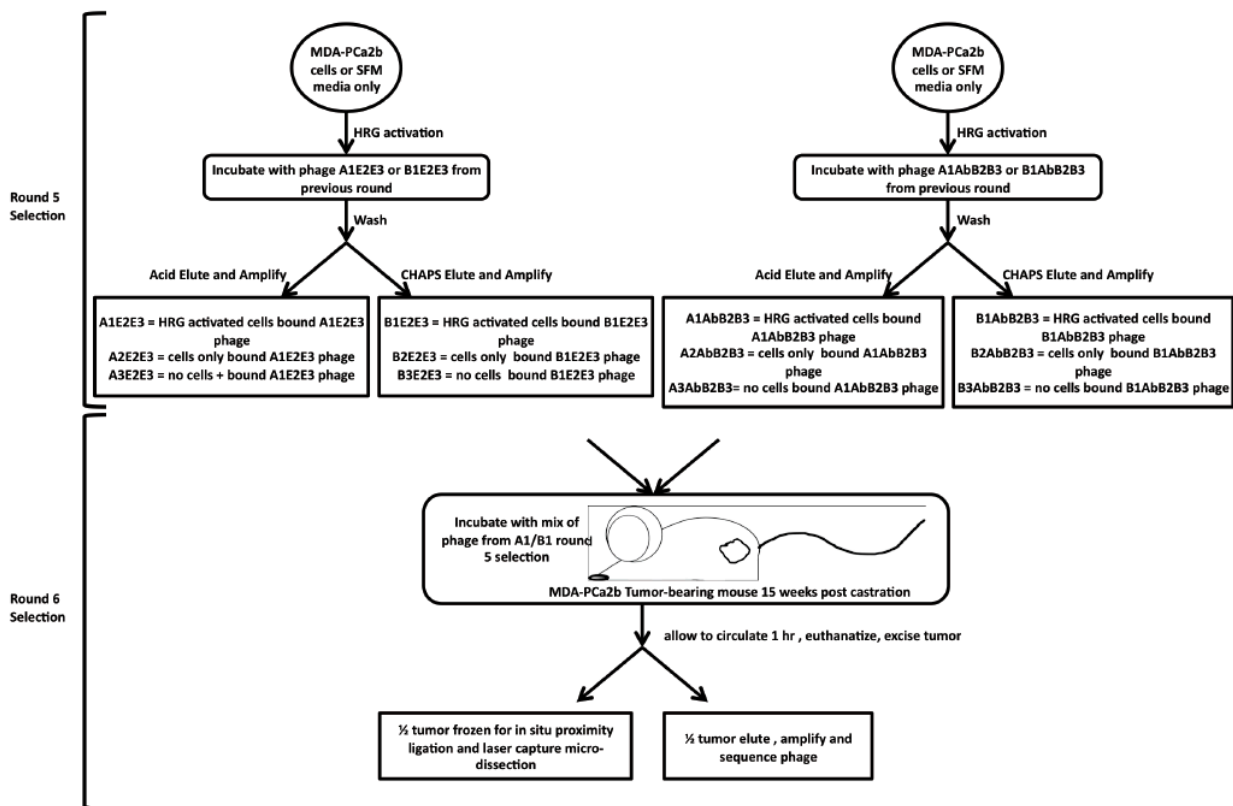


Figure 4. Fifth Round of Selection and In Vivo Selection. 5th round selection: In two 6 well plates (Row A and Row B on each plate, one plate for E2E3 selection and one for AbB2B3 selection), MDA-PCa2b cells plated in first 2 wells each row and last well each row had media only. Twenty four hours before selection, replace growth media with serum free media (SFM) in all six wells. In first wells of each row add HRG 100ng/mL for 10 minutes at 37°C. Remove all media from wells and replace with SFM containing 1012V/mL : in one plate A1 or B1E2E3 and in the other plate A1 or B1AbB2B3 . Incubate 30 minutes at 37°C. Wash 3X and elute phage. Acid elute top row in 800µL 0.1 N HCl, pH 2.2 with glycine for 10 min and neutralize. CHAPS elute bottom row in 1mL 2.5% CHAPS for 10 min. Keep each well eluate separate and amplify and purify phage as input for next round, saving cell pellets for RF DNA Extraction. Each subsequent round of selection will use the amplified, eluted phage from the previous round as input.

6th round selection: A1 and B1 phage from the 5th round, from both selection schemes, was mixed and injected into MDA-PCa2b tumor-bearing mice (n=2) 15 weeks post castration. The phage were allowed to circulate for 1 hour. Following euthanasia, tumors were excised and ½ tumor frozen for in situ proximity ligation and laser capture micro-dissection. The other ½ tumor was processed to elute amplify and sequence phage.

d. Perform in vivo phage display to isolate phage that posses both appropriate pharmacokinetics and affinity for ErbB2/ErbB3 heterodimer (months 4-7). The in vivo selection occurred in MDA-PCa-2b xenografted male nude mice. There was not enough phage in the tumor to perform laser capture dissection to isolate phage. The phage were obtained, rather, from tumor tissue homogenates. Progress: In vivo selection was performed as diagrammed in Figure 4.

e. Identification and analysis of selected peptide sequences using Next Generation sequencing – looking for sequence homology/motifs between the different selected phage populations (months 8-10).

Progress: Next Generation sequencing protocol was designed. After phage amplification the resultant E. coli pellet was processed for isolation of phagemid (phage plasmid) via midiprep. The purified phage DNA was then quantified and enzyme digested with NciI and EagI restriction enzymes. The digested phage DNA was then run on a 2.2% agarose gel and the approximately 350 base pair band of interest was excised and gel purified. After which time, the samples were submitted to the DNA core for DNA blunting and ligation of appropriate sequencing adapters. Select sequence output from the first five rounds of selection are shown in Table 1. As seen, several multiple hit sequences were found (color highlights). Underlined sequences contained shared amino acid motifs found in other sequences from these selections. The highlighted phage are being further analyzed for binding ErbB2/ErbB3.

Five rounds of in vitro phage display selection against ErbB2/B3 ECD heterodimer and MDA-PCa-2b cells, followed by a sixth round of in vivo phage display selection against castration resistant MDA-PCa-2b xenografted tumors was finished within the first year of this grant. However, the identification and analysis of the selected peptide sequences using Next Generation sequencing, as well as looking for sequence homology/motifs between the different selected phage populations was completed within the second year.

Table 1. ErbB2/ErbB3 Dimer Sequencing Results

selection		selection		selection		selection	
R5A1E23	1LVLPGRAYVVGSGV	R5B1E23	2ADAKIITGTAAYYLG	R5A1Ab	2LLATLSHLAYPSRAL	R5B1Ab	1PDIHVLPEFAHLGPG
R5A1E23	4SFWRVAVNYAYAPGA	R5B1E23	4PAVASTSSLIIDGPF	R5A1Ab	3LLSSGFLYPLYSTSS	R5B1Ab	2AGPVADAVDCGGILC
R5A1E23	5VGRVSPWIYRMTGV	R5B1E23	5NAVRVAFWSPLYPF	R5A1Ab	4AFLGSHWFPVAVSR	R5B1Ab	3RCVAHLSSRGGHDCG
R5A1E23	6GRDRFFFWFPLYDY	R5B1E23	6AISRATPLSVIHGVH	R5A1Ab	5RFWDYDMLRVLRLPL	R5B1Ab	4GCWELDFTRSWVHGC
R5A1E23	7GILLSEVFRSLTP	R5B1E23	7AAHVSEHYVSGSLRP	R5A1Ab	6RFWDYDMLRVLRLPL	R5B1Ab	5PLRPLLRCDDVSGSY
R5A1E23	9HFAGPLKYPSYSISS	R5B1E23	8RSCFVALPMCRGWGS	R5A1Ab	7AWVRGVFLRSPISSV	R5B1Ab	6TALFFPRDICKGLYS
R5A1E23	10SLYPLFVTRWSAGSG	R5B1E23	9GGWRSSFSDRVPPAF	R5A1Ab	8HSLFGAPWLEFSDHL	R5B1Ab	7SRFPASTLSWVPAWR
R5A1E23	12TKLFPVWRPAPGGVP	R5B1E23	10DPVCTFNADDAPTF	R5A1Ab	9TKLFPVWRPAPGGVP	R5B1Ab	8ARHWGLRPS
R5A1E23	13RSYSSSFVFSQGAFS	R5B1E23	11HGSLGLGWPGHTSVR	R5A1Ab	10LGFPIVSAHGPHIRS	R5B1Ab	9TAFVLGWSAFGRPPR
R5A1E23	14APNSAVLMFGTAYPS	R5B1E23	12GSSALPRNRTPSGII	R5A1Ab	11RFWDYDMLRVLRLPL	R5B1Ab	10SLTSLIPSPSPAAR
R5A1E23	16RGVAPFRWSPSLSS	R5B1E23	13ASSTGVPGYGYSGSD	R5A1Ab	12LLYSPGSSWAARQYM	R5B1Ab	12PSVLVRFVGLRLVTP
R5A1E23	17TKLFPVWRPAPGGVP	R5B1E23	14YVPASGLSGASWVLP	R5A1Ab	13RFWDYDMLRVLRLPL	R5B1Ab	13GLLPGSFVGGQAYWLP
R5A1E23	18GTLFLLRSLHASGLP	R5B1E23	17IMILLIFSLWFGGA	R5A1Ab	15PWLFVGGATKFGLL	R5B1Ab	14NAVRVAFWSPLYPF
R5A1E23	19VFGTSLGPRAGDV	R5B1E23	18IKPGSSATHTFSPYR	R5A1Ab	16FHRVSPLLGREFAH	R5B1Ab	15SFRYPRIISFDPSAT
R5A1E23	21VVLFPALYHSSVYGS	R5B1E23	19RLSHSIFELAPVSTP	R5A1Ab	17REFAHFHGSRSAFPF	R5B1Ab	16LKSVDVFPDHPVR
R5A1E23	23RWLARYWAGWHLPGF	R5B1E23	20PFVPTASSWALDLP	R5A1Ab	18VFPLRVDCEFCVSGL	R5B1Ab	17TGPESVSGGMRFGG
R5A1E23	24HGSLGLGWPGHTSVR	R5B1E23	22ILGSPAGFFRYPLTL	R5A1Ab	20CVDCYPWSRDLTRDS	R5B1Ab	18GLLPGSFVGGQAYWLP
		R5B1E23	23PLDFHGAHSRGRSRV	R5A1Ab	21SFFGVWPFARHLGAS	R5B1Ab	20TFTRVTVDVYGRRLS
		R5B1E23	24RGGFSDTSRTGWVSV	R5A1Ab	22FLGPTLAKMVARARM	R5B1Ab	21RMRLSPIGFFGSRVP
						R5B1Ab	22ARFLSSTRSPSVSVS
						R5B1Ab	23SVYDVFTRGTNRGRV

Sequences from 5th round of fUSE5 selection with PCa2b cells. Highlighted were multiple hits in these selections. 5 rounds of selections: 2 against PCa2b cells, 2 against either ErbB2/ErbB3 (E2) or AbB2B3HRG (Ab), 1 selection against PCa2b cells.

R5A1E2 = 4th round E2/E3 immobilized protein phage selected against HRG activated cells and eluted with acid;
R5B1E2=4th round E2/E3 immobilized protein phage selected against HRG activated cells and eluted with CHAPs;
R5A1Ab=4th round Ab captured HRG E2/E3 protein phage selected against cells and eluted with acid;
R5B1Ab=4th round Ab captured HRG E2/E3 protein phage selected against cells and eluted with CHAPs.

The Next Generation sequencing protocol designed in year 1 was utilized, in short, after phage amplification the resultant E. coli pellet was processed for isolation of phagemid (phage plasmid) via midiprep. The purified phage DNA was then quantified and enzyme digested with NciI and EagI restriction enzymes. The digested phage DNA was then run on a 2.2% agarose gel and the approximately 350 base pair band of interest was excised and gel purified. After which time, the samples were submitted to the DNA core for DNA blunting and ligation of appropriate sequencing adapters. Subsequently, the phage genome

sequence was removed from the sequence of interest (foreign displayed peptide), the total number of unique peptide sequences identified, and the frequency of each sequence determined for Round 6 (R6), Round 5 antibody immobilized ErbB2/B3 ECD heterodimer (R5AbB2B3), Round 5 equal molar mixture of B2 and B3 (R5B2B3), Round 5 MDA-PCa-2b cell binding (R5 Cell Binding), plastic binding, and Naïve library. We found a total of 3265, 12910, 11694, 48325, 6276, and 116404 unique sequences within each sample group, respectively. Table 1 contains the top 25 ranked sequences identified within R6. Ranking is determined by the number of matching peptide sequences identified. The rank and frequency of each phage display selected sequence was then determined for each of the phage display parameters probed (Table 2). The large number of unique sequences identified within many of the sample sets suggests either a lack of selective pressure or complex samples with many potential binding sites. However the final in vivo round of selection within nude mice bearing castration resistant human prostate carcinoma MDA-PCa-2b xenograft tumors significantly reduced the total number of unique sequences revealing the stringency of an in vivo selection protocol.

Table 2. The Top 25 Sequences from the 6th Round of fUSE5 Selection within a Castrated, Nude Mouse Bearing a MDA-PCa-2b Castration Resistant Tumor.

Sequence	R6	R5AbB2B3	R5B2B3	R5 Cell Binding	Plastic Only	Naïve Library	Cluster or Motif
RLWFALAFFLGLCPM	1-667	16-670	288-17	563-91	N/A	2313-14	Yes
PFARAPVEHHDVVGL	2-364	123-95	5-500	6-4077	35-15	102-152	No
SLLFLRSWPKTLAGV	4-189	2-1537	1-1434	1-17163	839-2	661-40	Yes
GLLPGSFVQAYWLP	3-193	24-558	15-195	18-2349	252-3	698-38	No
RVPPRYHAKISPMVK	5-158	89-140	13-207	30-1822	71-8	345-69	No
PAVASTSSLIIDGPF	6-156	480-18	28-140	82-806	61-9	69-212	No
DRARPDRCRSWGICP	7-147	68-183	2988-2	2011-21	N/A	58241-1	No
SLAPYSLRILRVGSA	8-138	11-818	3-670	2-11676	232-3	418-61	No
GPGSFVPVAFRPGPF	10-131	N/A	115-48	725-69	666-2	1059-27	No
PIFVVSSSGSSSSP	9-131	201-53	58-89	102-676	823-2	306-75	No
RGGRCLLCLLWWA	11-129	473-18	88-64	174-355	200-4	135-130	Yes
PKAFQYGGRAVGGLW	12-127	95-134	6-485	12-3156	9-46	2-2712	No
VWWRALLVFATLYSV	13-125	219-47	49-105	148-450	36-14	33-407	No
GFTDVHLHLPGNHR	14-119	276-34	18-192	29-1830	53-10	140-129	No
AREYGTRFSLIGGYR	15-114	19-649	4-536	5-4665	2-112	1-3436	Yes
AVAGGRSVVDARVAR	16-107	527-16	63-82	88-780	189-4	77-191	No
LGRAGQSYPSFARGL	17-81	228-44	44-111	50-1193	985-1	156-117	No
ERDPRHVHRSGSAIG	18-74	4044-2	142-37	5287-7	N/A	36683-1	No
RFWDYDLMLRVLRPL	19-73	1-4548	188-27	3-9320	162-4	80-182	Yes
GCSALVGFLLCCM	20-73	140-85	60-84	65-1014	793-2	90-165	No
GSAFLYAVLRNVSSR	21-72	73-170	20-181	16-2766	2248-1	2088-16	No
VVSSRSVLSSQYRGH	22-69	132-90	65-81	64-1036	341-3	84-172	No
REFAHFHGSRSAFPF	24-64	3-1497	915-6	14-2792	N/A	53792-1	Yes
EPYGFIAFSRAAHSP	23-65	4-1287	12-224	10-3269	409-2	181-109	Yes
WRRWFYQFPTPLAAA	25-63	15-696	2-897	4-8917	N/A	58807-1	No

The ranking and total number of identical sequences for each sequence is listed (rank - # of hits). Dark green and dark red highlighted cells identify sequences found 500 times or more. While light green and light red highlighted cells identify sequences found 100 – 499 times.

Further analysis of the page display selected peptide sequences was performed by the University of Missouri Bioinformatics Core. Bioinformatics algorithms revealed sequence clusters within both Round 5 sequence output and Round 6 sequence output (Figure 5). Clusters of sequences are defined as groups of homologous peptide sequences that are clustered in order to generate a list of non-redundant representative sequences. Interestingly R5AbB2B3 sequence output resulted in 8 sequence clusters that were all 15 amino acids in length, while the R6 sequence output gave rise to 9 sequence clusters that ranged in length from 8 to 15 amino acids in length. These lists of unique and clustered sequences were then utilized within a motif discovery algorithm called “Multiple Em for Motif Elicitation” (MEME) (1).

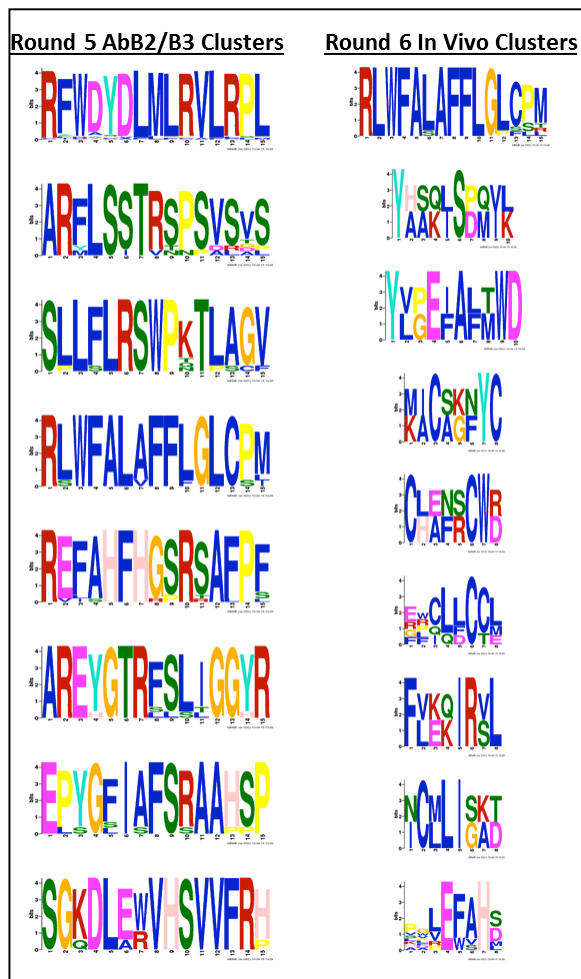


Figure 5. Sequence Clusters from R5AbB2B3 and R6 samples.

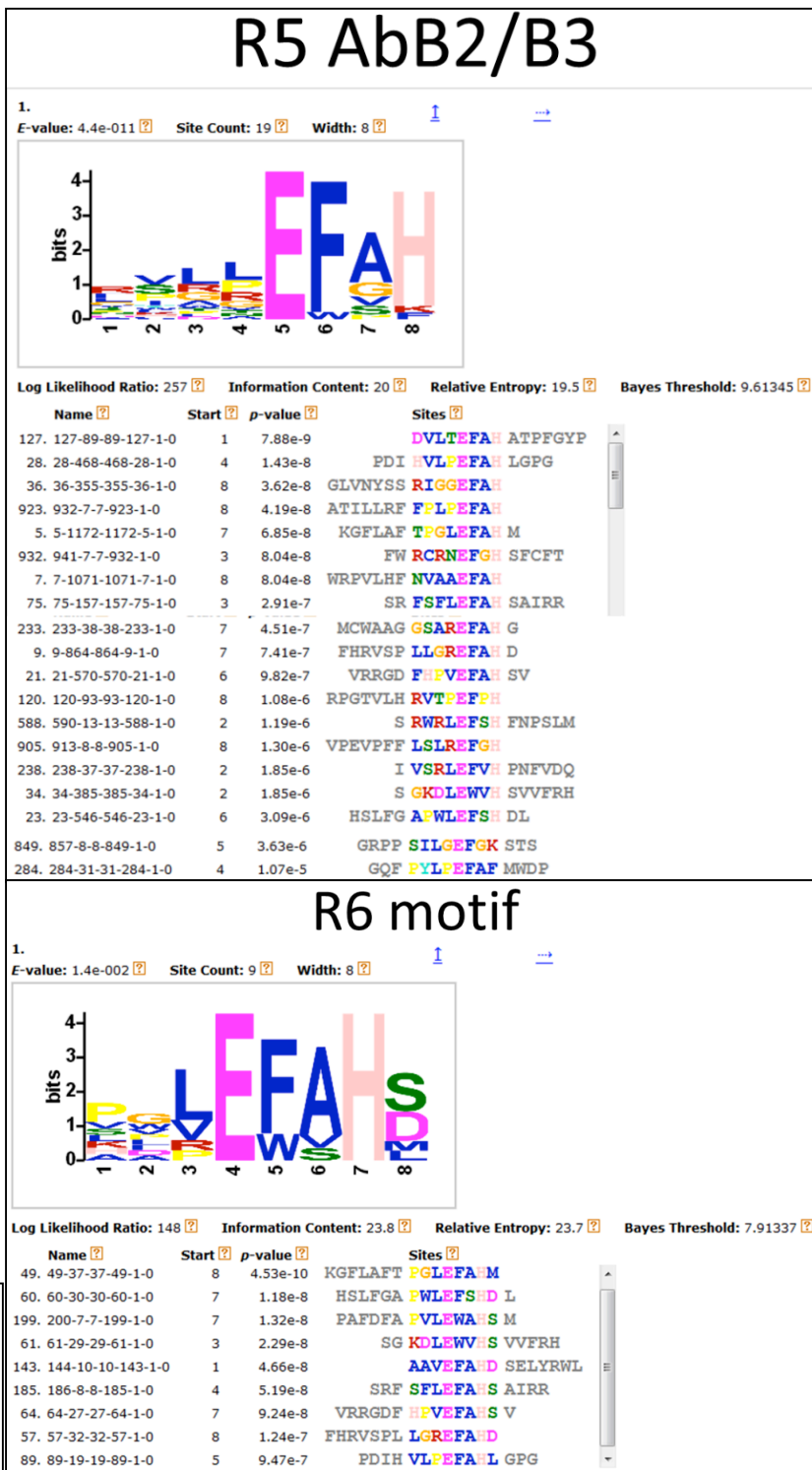


Figure 6. Sequence Motifs from R5AbB2B3 and R6 samples. The clustered sequence lists of R5AbB2B3 and R6 were submitted to the MEME algorithm for discovery of un-gapped motifs.

MEME searches for recurring, un-gapped motifs as shown in Figure 6. The main motif produced by the MEME algorithm within both R5AbB2B3 and R6 samples sets contained ...EFAH.. core sequence. R5AbB2B3 sample contained 19 sequences with this core consensus, while the R6 sample contained only 9 peptides with this motif. Sequences containing high value motifs or clusters with 3 or more sequence variants are highlighted dark green in Table 2.

Task 2. In Vitro Characterization of Selected Phage Clones and QDs Conjugated to Selected Peptides (months 11-19)

Subtask 2a and 2b. The binding affinity and specificity of individual selected phage clones for ErbB2/ErbB3 heterodimer will be determined.

Progress: 2a. The top 25 phage clones identified were first cleared of phage clones with known growth advantages (PFARAPVEHHDVVGL), phage clones with over representation within the naïve library (PKAFQYGGRAVGGLW and AREYGTRFSLIGGYR), and phage clones that were previously identified in other unrelated phage display selections performed within this laboratory (PIFPVVSSSGSSSSP and SLAPYSLRILRVGSA). The remaining 20 phage clones were then utilized within a phage capture ELISA assay to for validation of each selected phage clone (Figure 7). 16 phage clones of the 20 tested had a ratio of 5 or higher for B2/B3 heterodimer binding to no protein binding. In order to further narrow the number of hits, this data was then compared back to the Next Generation sequence data and the cluster and motif data. We then selected the phage clones that 1) were represented within a cluster and/or motif, 2) had high frequency within the R5AbB2B3 Next Generation sequencing data, and 3) a ratio of B2B3 heterodimer binding to no protein binding of 5 or higher. There were 9 phage clones that matched these criteria. These 9 phage displayed peptide sequences were then synthesized as biotinylated peptides for further analysis of B2/B3 heterodimer binding.

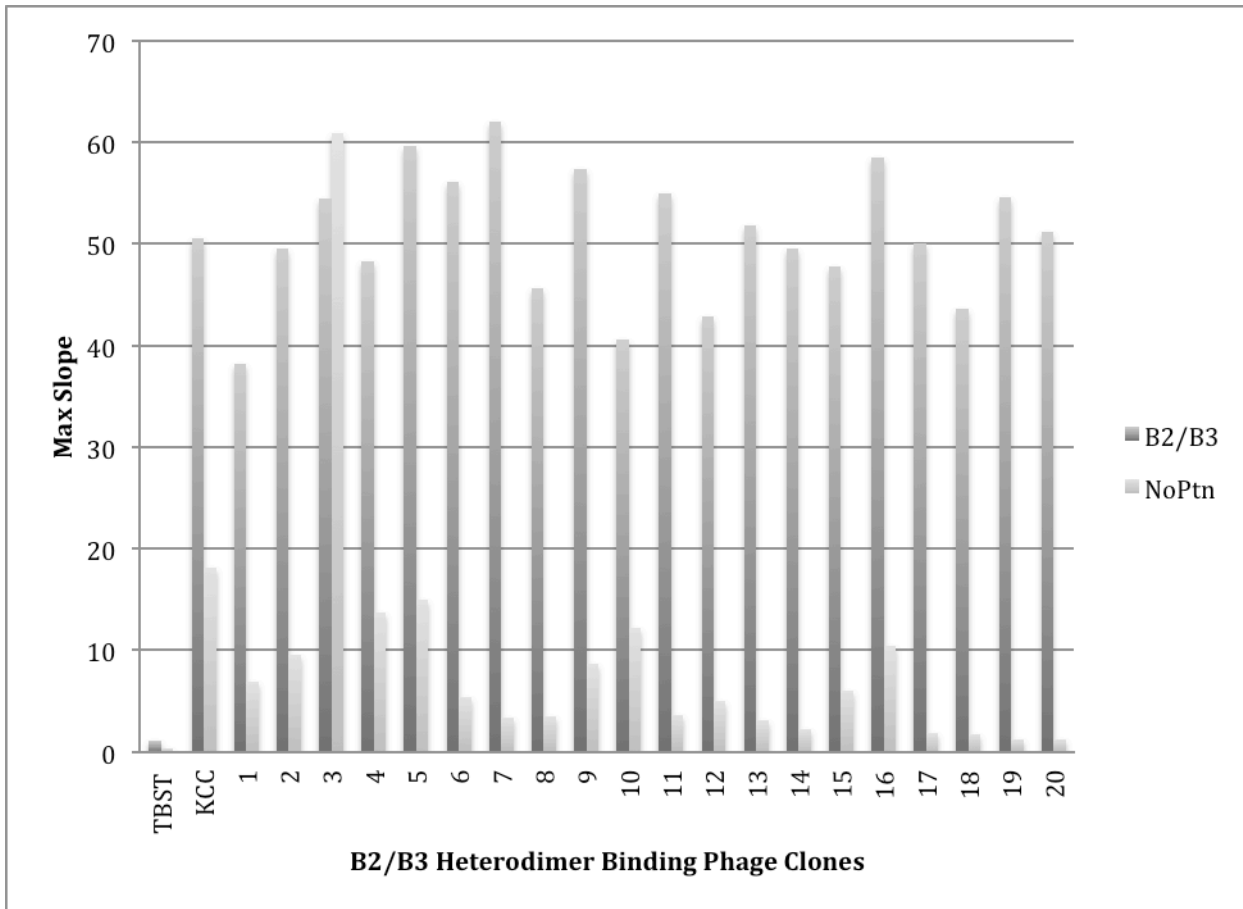


Figure 7. Phage capture ELISA. The top 20 phage clones resulting from the phage display selection and sequence analysis were tested for their ability to bind to immobilized B2/B3 ECD heterodimer. 96 well ELISA plate was coated with 50ng of ErbB2 ECD mixed with 50ng of ErbB3 ECD overnight at 4°C. The plate was then washed and blocked with synthetic blocking buffer for 2 hours at room temperature. 5×10^{10} virion/well of phage clone was added to the wells and incubated at room temperature for 1 hour. After washing the bound phage was detected with a polyclonal anti-phage antibody and appropriate secondary conjugated to HRP. HRP substrate [2,2-azino-bis(3-ethylbenzothiazoline-6-sulfonic acid)] was added, allowed to develop at room temperature within the plate reader for continuous quantification over a period of 20 minutes by measuring the absorbance at 405 nm.

2b. The binding specificity of individual selected phage clones for native ErbB2/ErbB3 heterodimer within live prostate carcinoma cell lines will be determined. Followed by analysis of affinity for prostate carcinoma cells displaying native ErbB2/ErbB3 heterodimer (month 13-14).
 Progress: Proximity ligation assays were performed to examine ErbB2/ErbB3 heterodimer formation. As shown in Figure 8 there was marked increase in ErbB2/ErbB3 heterodimer with addition of HRG (as shown in red in lower left panel).

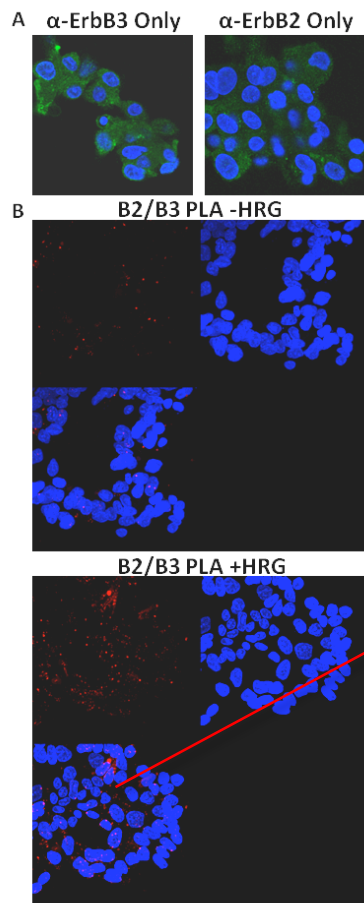
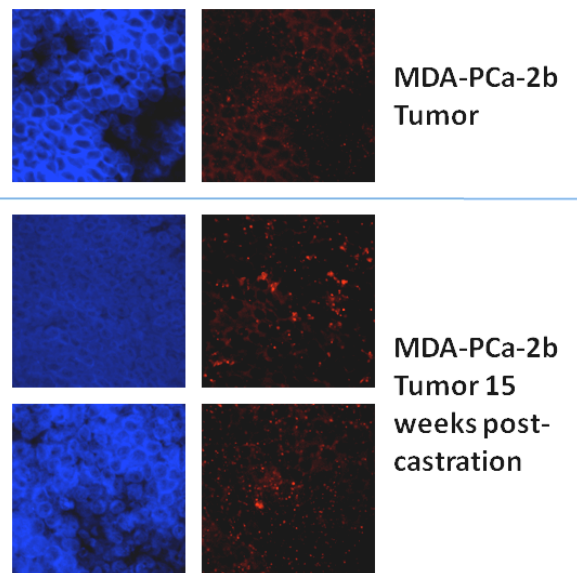


Figure 8. ErbB2, ErbB3, and ErbB2/B3 heterodimer on MDA-PCa-2b cells. MDA-PCa-2b cells were grown on tissue culture treated glass slides. The media was removed, cells gently washed, and then fixed in 10% buffered formalin for 30 minutes at 37°C. (A) Presence of ErbB2 and ErbB3 on the cell surface of MDA-PCa-2b cells was confirmed using antibodies specific for each receptor and an appropriate FITC labeled secondary antibody (green). (B) MDA-PCa-2b cells were serum starved for 24 hours then received a 15 minute treatment of 100ng/mL of HRG (bottom panel) or PBS only (middle panel) prior to washing and fixation. Matched pair antibodies specific for ErbB2 and ErbB3 were utilized in a PLA signal amplification protocol (red). Cells were then imaged using a z-stacking technique in which 25 slices (images) were merged into 1 image. The resulting image contains B2/B3 PLA signal from many focal planes. Lower left image is DNA staining (blue) and merged ErbB2/ErbB3 heterodimer (red).

Heterodimer

The existence of ErbB2/ErbB3 heterodimer was also verified in MDA-PCa-2b prostate tumor tissue from xenografted castrated mice (Figure 9). These studies show ErbB2/ErbB3 heterodimer formation is increased upon HRG treatment and in hormone resistant tumors.

Figure 9. B2/B3 heterodimer occurrence in MDA-PCa-2b xenografted tumors. MDA-PCa-2b tumors resected from non-castrated mice at 14 weeks post-inoculation and tumors from castrated mice 15 weeks post-castration were probed for B2/B3 heterodimers (top panel) using the PLA technique. PLA signal from the B2/B3 heterodimer is shown as red.



c. Synthesize the anti-TF peptide (P30-1) and ErbB2/ErbB3 heterodimer targeting peptides for covalent conjugation to QDs (month 15).
 Progress: TF targeting P30-1, ErbB2 targeting KCCYSL, and ErbB3 targeting MSP3 have been synthesized for conjugation to QDs.

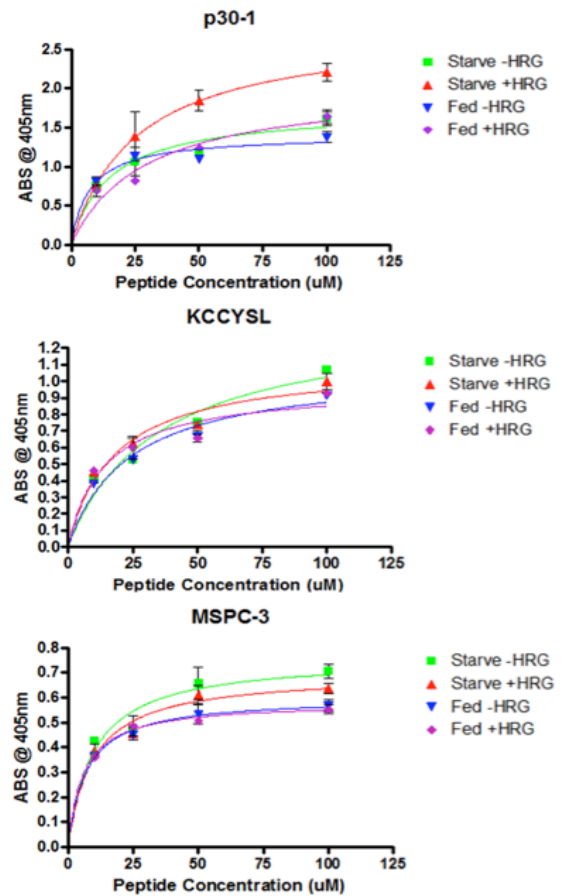
d. In vitro characterize ErbB2/ErbB3 heterodimer binding of five different phage display selected peptide-QD conjugates and five scrambled peptide-QD conjugates (month 16-17).

Progress: Completed

e. In vitro characterize TF binding of the p30-1-QD conjugate and scrambled p30-1-QD conjugate (month 16-17).

Progress: TF targeting P30-1, ErbB2 targeting KCCYSL, and ErbB3 targeting MSP3 peptides were conjugated to QDs and their binding to MDA-PCa-2b prostate cancer cells was analyzed with and without the presence of HRG (Figure 10). As shown, ErbB-2 and ErbB3 peptides alone do not exhibit increased binding to the prostate cancer cells in the presence of HRG, whereas the TF-binding peptide does. Thus, KCCYSL and MP3 serve as negative controls for ErbB2/ErbB3 heterodimerization.

Figure 10. Binding of biotinylated peptide to MDA-PCa-2b cells. MDA-PCa-2b cells were grown to 80% confluence in 96 well plates. The cells were then serum starved for 24 hours followed by a 15 minute treatment of either 100ng/mL HRG or PBS only. The media was removed and biotinylated peptide in PBS added to the cells for a 30 minute incubation. After which time the cells were washed and fixed in 10% buffered formalin for 30 minutes. The fixative was then washed away and presence of biotinylated peptide probed with streptavidin-HRP.



f. Characterize binding patterns of QDs conjugated to anti-TF p30-1 peptide, scrambled p30-1, anti-ErbB2/ErbB3 heterodimer peptides, and corresponding scrambled peptides to prostate carcinoma cell lines as well as benign immortalized prostatic cell lines (month 18).

Progress: Due to problems with the synthesis of all the 9 peptides, we initially probed the binding of 8 biotinylated peptides to human prostate carcinoma MDA-PCa-2b (B2+ and B3+) and PC-3 cells (B2+ and B3-) (Figure 11,12). Of the 8 biotinylated peptides tested, 2 peptides, #3 and #4, displayed lowered cell binding in serum starved cells and increased cell binding to cells treated with HRG. Presumably, this cell binding pattern would be due to formation of B2/B3 heterodimer upon activation with HRG. This data is not entirely unexpected, there are many instances of phage display selected peptides that bind to their intended target when displayed upon the surface of the phage particle but that lose function when synthesized as a free peptide. These two peptides were then further investigated with a proximity ligation assay (PLA) to stain native B2/B3 heterodimer in combination with the B2/B3#3 and B2/B3#4 for dual staining of B2/B3 heterodimer (Figure 13). In this assay only the peptide B2/B3#3 generated fluorescent signal that colocalized with the PLA B2/B3 heterodimer fluorescent signal. Next, the two top peptides (B2/B3#3 and B2/B3#4) as well as the newly synthesized B2/B3#9 peptide cell binding were utilized in another cell binding experiment to probe the binding propensity of each peptide to B2, B3, and/or B2/B3. Thus, binding of each peptide to cells with various levels of expression of either B2 or B3 was compared to the binding propensity of each peptide to cells overexpressing both B2 and B3 (Figure 8). The three phage display selected anti-B2/B3 heterodimer peptides bound highest to MDA-PCa-2b and MDA-MB-435 cells, both of which overexpress both ErbB2 and ErbB3. While the anti-ErbB3 peptide, MSP3, bound to MDA-MB-361

and MDA-MB-435 the brightest. To further quantify the binding of our three phage display selected anti-B2/B3 heterodimer peptides we next performed a series of cell based ELISAs (Figure 14). A pattern of binding is discernable in Figure 14. Peptides specific for ErbB2 or ErbB3 generally have higher cell binding to cell that were not treated with HRG, while peptides that bind to ErbB2/B3 heterodimer have higher binding to cells that have received HRG treatment. An exception to this observation is that of B2/B3#4 peptide. This peptide seems to bind to all cell lines irrespective of the expression levels of ErbB2 and/or ErbB3. Thus we continued investigation of the ErbB2/B3 heterodimer specificity of B2/B3#3 (REFAHFHGSRSAFPF) and B2/B3#9 (RLWFALAFFLGLCPM).

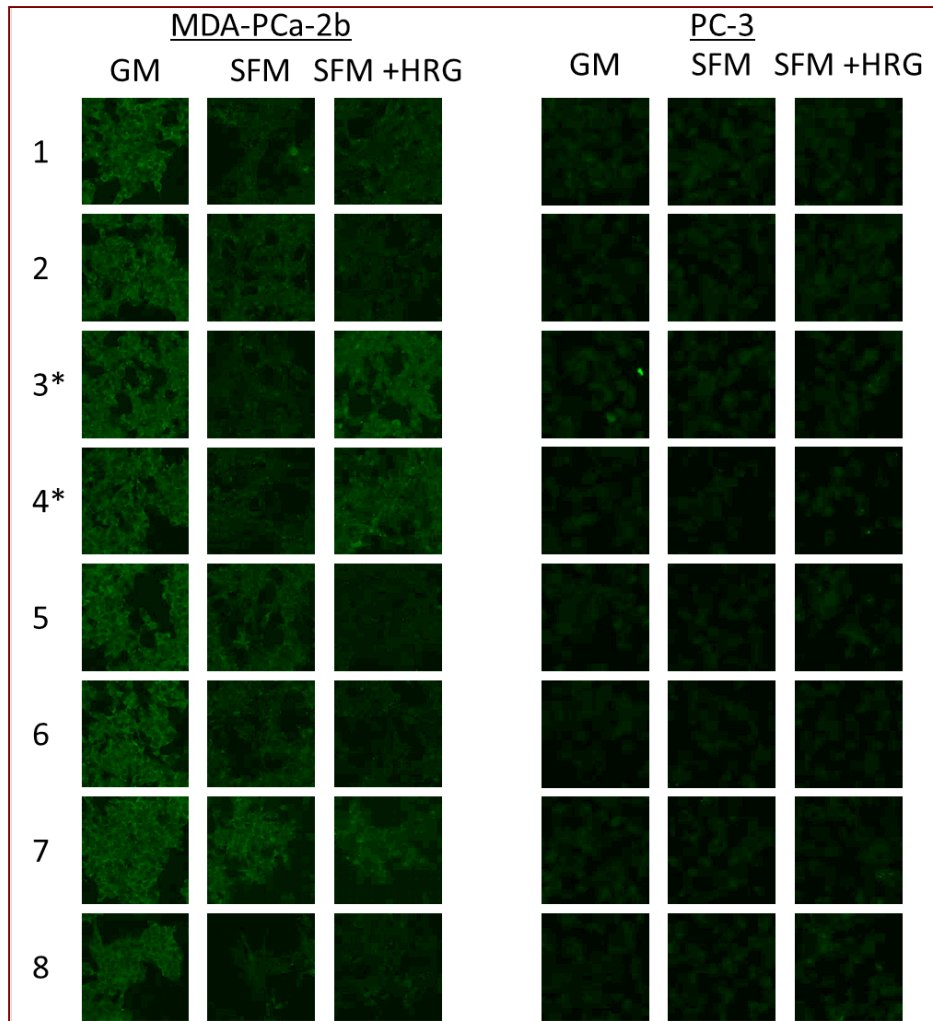


Figure 11. Cell Binding of Synthesized Biotinylated anti-B2/B3 Phage Display Selected Peptides. MDA-PCa-2b and PC-3 cells were grown on microscope slides. 24 hours prior to the peptide binding experiment, cell growth media was replaced with either fresh growth media (GM) or serum free media (SFM). 30 minutes prior to the peptide cell binding experiment serum starved cells were treated with 100ng/mL HRG in SFM. Next, 50 μ M biotinylated peptide was incubated with cells for 30 minutes at 37°C. After which cells were fixed with 10% buffered formalin. The fixed cells were then rinsed and blocked with 5% BSA in PBS for 2 hours at room temperature. Finally, the cells were incubated with streptavidin-Oregon Green conjugate for 1 hour at room temperature, washed, and slide cover mounted. The presence of cell bound biotinylated peptide/fluorescent streptavidin complex was probed using a Leica confocal microscope.

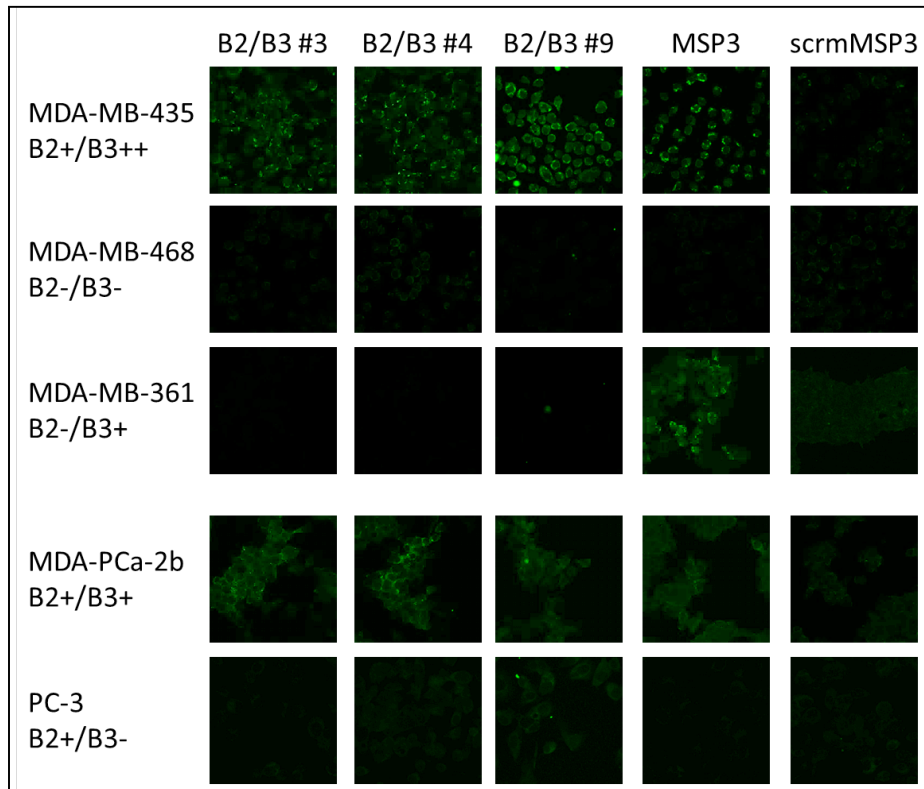


Figure 12. Cell Binding of Biotinylated Anti-B2/B3 Phage Display Selected Peptides to a Panel of Human Carcinoma Cell Lines. Biotinylated B2/B3#3 and B2/B3#4, along with the newly synthesized B2/B3#9 were utilized in a cell binding experiment with various human carcinoma cell lines that were both serum starved and HRG treated as described in Figure 4.

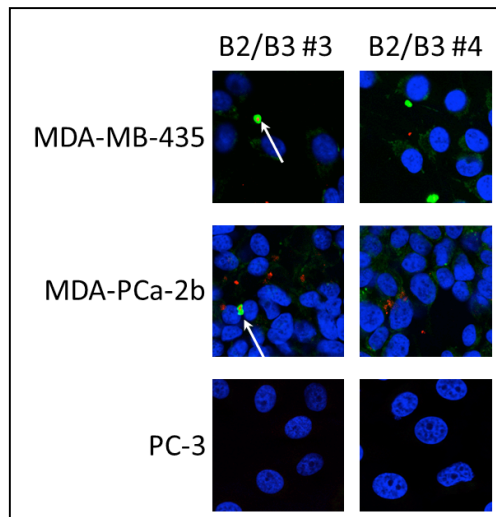


Figure 13. Binding of Biotinylated Anti-B2/B3 Selected Peptides to Native B2/B3 Heterodimer on Human Carcinoma Cell Lines. The images of B2/B3#3 and B2/B3#4 (green) bound to the surface of B2/B3+ cell lines that were treated with SFM and HRG (as described in Figure 4) were overlaid with the PLA signals (red). And the nuclei were counter stained blue. White arrows indicate co-localized PLA/peptide signals.

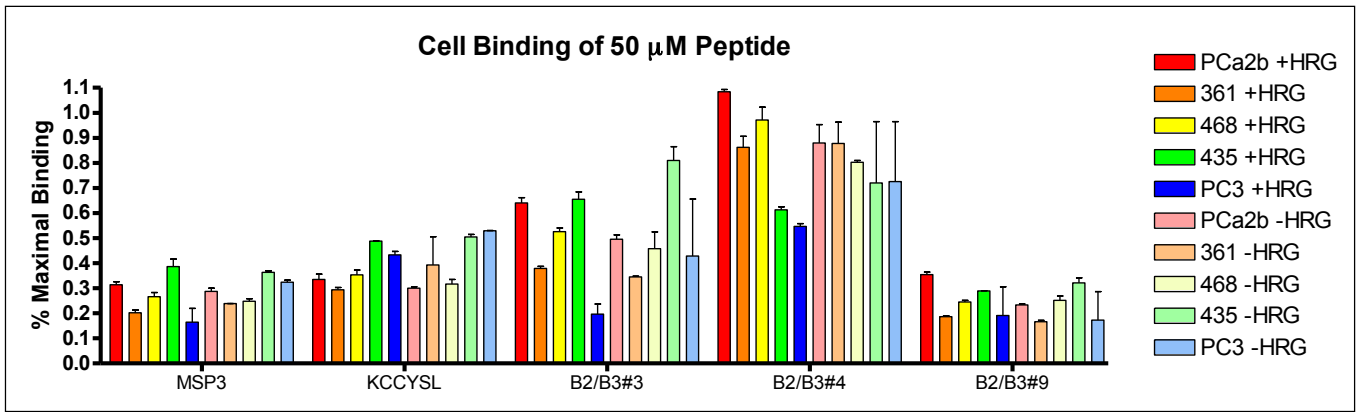


Figure 14. Binding of Biotinylated Peptides to Human Carcinoma Cell Lines. A panel of human carcinoma cell lines with varying levels of ErbB-2 and ErbB-3 expression was utilized to probe the specificity of peptide binding. Cells were grown in tissue culture treated 96 well plates to 80% confluency. The cells were then serum starved for 24 hours. One half of the cells were then stimulated with 100 ng/mL of HRG for 30 minutes, followed by incubation with the biotinylated peptide for 30 minutes at 37°C. After which time the cells were washed with ice cold PBS and fixed with 10% buffered formalin overnight at 4°C. The next day, the cells were washed, blocked, and incubated with streptavidin-HRP for the quantification of bound peptide.

To confirm the ability of B2/B3#3 and B2/B3#9 peptides to specifically bind to B2/B3 heterodimer we next utilized these peptides in an ELISA with purified, recombinant ErbB2 ECD and ErbB3 ECD (Figure 15). We probed the ability of peptides to bind to ErbB2 ECD, ErbB3 ECD, an equal mixture of the two ECDs and an Ab immobilized HRG/B2/B3 complex (AbB2B3). Interestingly, the anti-ErbB3 peptide, MSP3, again bound ErbB3 ECD the best with moderate binding to ErbB2 ECD and significantly lower binding to AbB2B3. In comparison, KCCYSL and B2/B3#3, an ErbB2 targeting peptide and a B2/B3 heterodimer targeting peptide, respectively, seemed to bind all samples similarly. Importantly, B2/B3#9 bound highest to Ab immobilized HRG/B2/B3 complex with very low binding to individual or mixed Erb ECDs. To further analyze peptide binding to AbB2B3 we performed an ELISA with dilution series of peptide to determine the maximal binding of each peptide (Figure 16). B2/B3#3 and B2/B3#9 had the highest binding values of 1.71 μM and 1.08 μM, respectively. In comparison, MSP3 and KCCYSL B_{max} values were less than half of the phage display selected anti-B2/B3 heterodimer peptides.

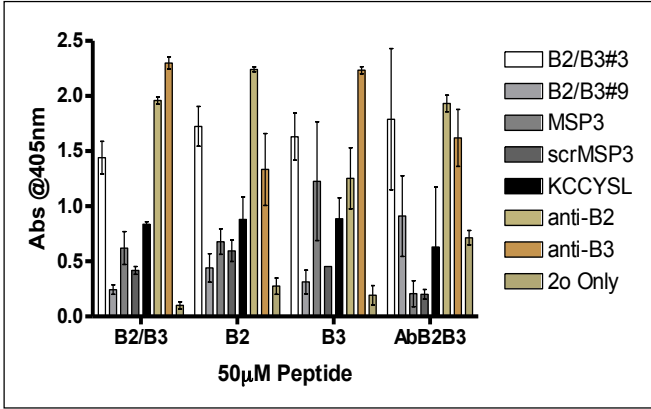


Figure 15. Binding of Biotinylated Peptides to Purified Erb ECDs and ErbB2/B3 Heterodimer. Purified, recombinant ErbB2 ECD, ErbB3 ECD or anti-ErbB3 Ab was coated overnight in a 96 well plate. Wells were washed, blocked and pre-incubated HRG/ErbB2/ErbB3 captured within the wells coated with Ab. The plate was then washed and incubated with either antibody or biotinylated peptide. Bound peptide or antibody was detected with a secondary HRP conjugate.

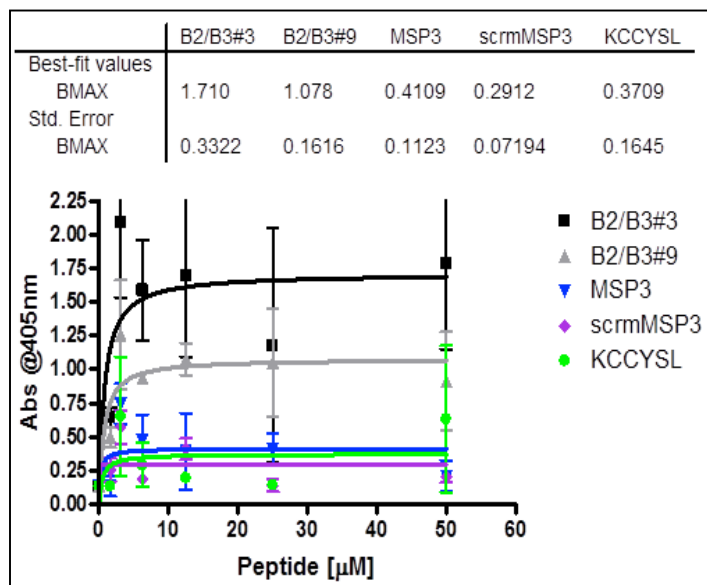


Figure 16. Binding of Biotinylated Peptides to Purified ErbB2/B3 Heterodimer. Anti-ErbB3 Ab was coated overnight on a 96 well plate. Wells were washed, blocked and pre-incubated HRG/ErbB2/ErbB3 captured. The plate was washed and incubated with peptide or Ab. After washing the wells were incubated with HRP conjugated secondary, washed again and the plate developed.

Next, we complexed biotinylated peptide to streptavidin coated Qdots for the analysis of molecularly targeted Qdots. Unfortunately, the presence of both lysines and cysteines within various peptides (especially KCCYSL) prevented successful covalent attachment of the peptides to a Qdot. Thus, the synthesized biotinylated peptide/Qdot complexes were used for fluorescence optical imaging of human carcinoma tissue cultured cells (Figure 17). Interestingly, the levels of fluorescent signal from KCCYSL, MSP3, B2/B3#3, and B2/B3#9 peptide/Qdot complexes were much more similar than that determined for biotinylated peptide alone. This could be attributed to an avidity effect of complexing multiple peptides to a single Qdot.

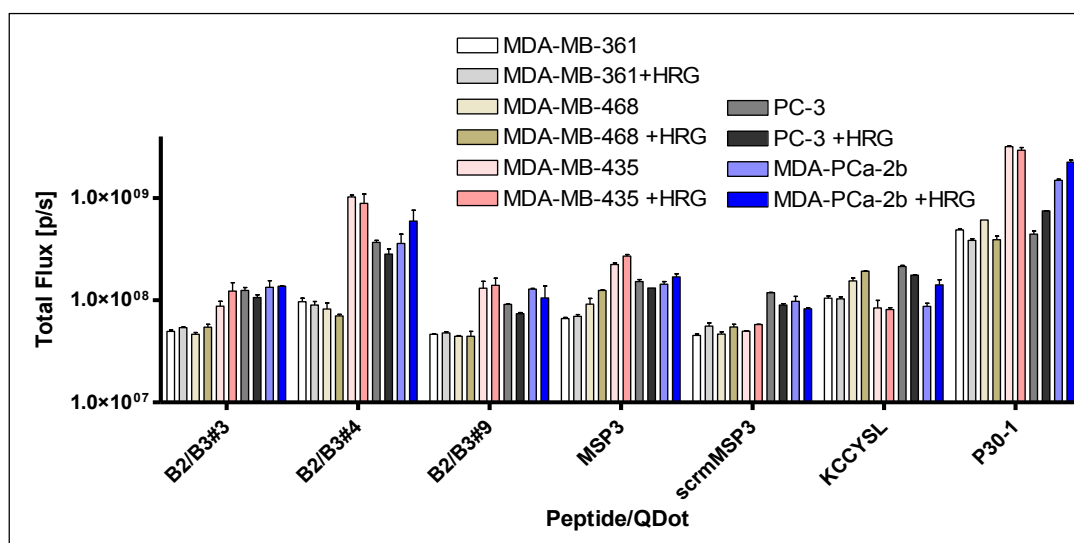


Figure 17. Binding of Peptides/Qdot Complexes to Human Carcinoma Cell Lines. Anti-B2, anti-B3, and anti-B2/B3 peptides were complexed with Qdot for the optical detection of cell binding. Human carcinoma cells were grown in 48 well plates and serum starved for 24 hours. One half of the cells were then treated with 100 ng/mL HRG for 30 minutes. The peptide/Qdot complexes were then incubated for 30 minutes at 37°C, washed with ice cold PBS, and imaged using an IVIS Spectrum (PerkinElmer).

g. Perform CRET imaging in vitro with molecularly targeted QDs bound to live human prostate carcinoma cell lines in the presence of ^{18}F -fluorocholine (month 19).

Progress: We used 18-FDG for imaging but were not able to synthesize 18F-choline. We produced CRET signals using Qdot-705 and 18-FDG. Figure 18 demonstrates the effects of varying the exposure time use of different filter sets upon the signal output of fluorescence and luminescent imaging of Cerenkov radiation production. From this data we determined the appropriate filter sets and image acquisition times. Fluorescent excitation of 500 ± 15 nm and fluorescent emission of 700 ± 10 nm with a 1 second image acquisition for Qdot-705 imaging was optimal. In comparison, no excitation or emission filters with an acquisition time of 300 seconds for Cerenkov imaging.

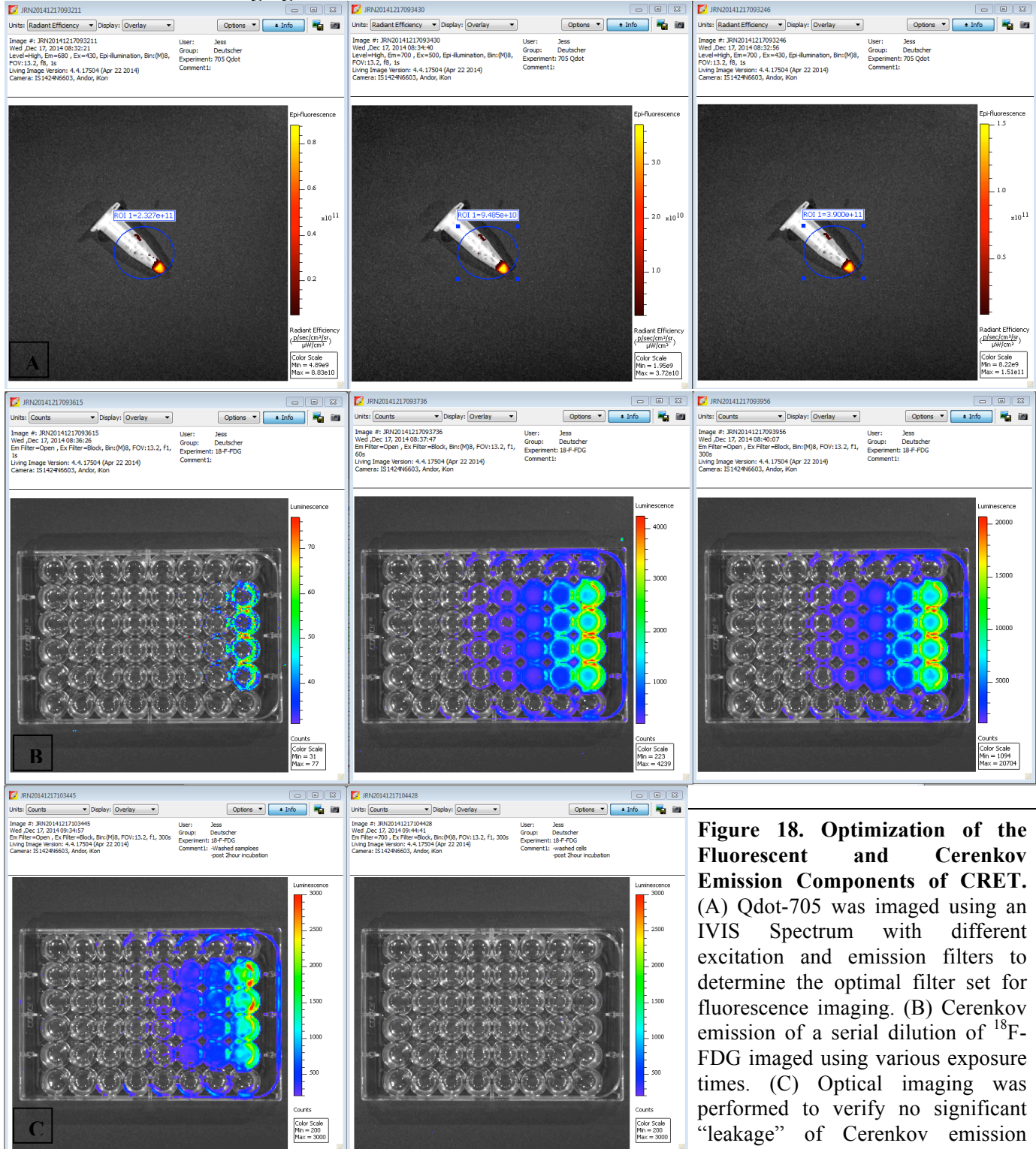


Figure 18. Optimization of the Fluorescent and Cerenkov Emission Components of CRET. (A) Qdot-705 was imaged using an IVIS Spectrum with different excitation and emission filters to determine the optimal filter set for fluorescence imaging. (B) Cerenkov emission of a serial dilution of ^{18}F -FDG imaged using various exposure times. (C) Optical imaging was performed to verify no significant "leakage" of Cerenkov emission within the 700 bandpass emission filter selected for CRET imaging.

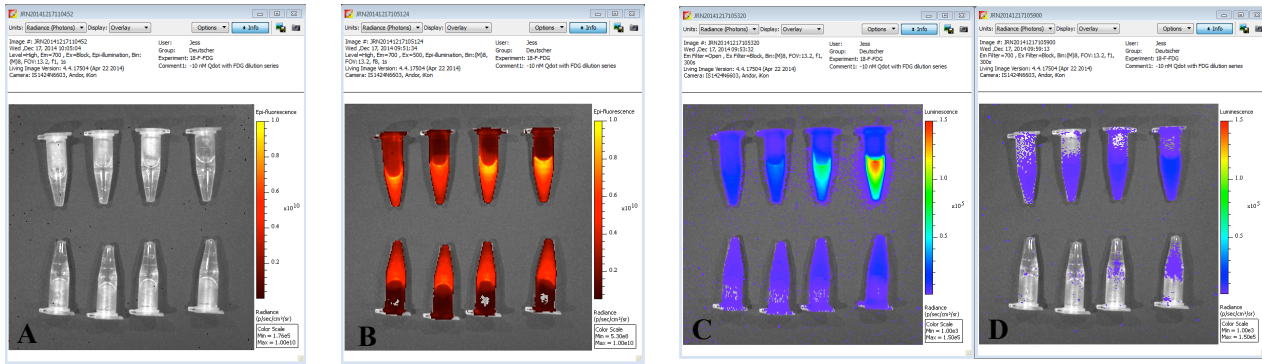


Figure 19. Optical Imaging of Cerenkov Energy Transfer. (A) Optical image of 8 tubes of 10 nM Qdot-705 using the CRET imaging filter set. (B) Fluorescent imaging of 8 tubes containing 10 nM Qdot-705 in PBS. (C) Open filter set for the imaging of a serial dilution of ^{18}F FDG Cerenkov emission containing 250, 125, 62.5, 31.3, 15, 7.5, 3.75, or 1.8 $\mu\text{Ci}/100\text{uL}$. (D) CRET signal from 10 nM Qdot samples with serial dilution of ^{18}F FDG.

CRET imaging of Qdot-705 and 18-FDG is shown in Figure 19. To verify there was no autofluorescence within the predetermined image acquisition parameters, tubes containing a 10 nM solution of Qdot-705 were imaged using the blocked excitation (ie. No excitation) and $700 \pm 10\text{nm}$ emission filter set. We also verified that the luminescent imaging of Cerenkov radiation did not overlap with the $700 \pm 10\text{nm}$ emission filter set (Figure 18c). To these tubes of 10 nM Qdot and serial dilution of 18-FDG was added followed by the acquisition of a Cerenkov radiation luminescent image and a CRET image.

Task 3. Optimize Components of CRET Imaging in the Prostate Carcinoma Tumor Model MDA-PCa-2b

Subtask 3a: Inoculation and castration of nude mice to generate the MDA-PCa-2b human xenograft model of prostate carcinoma progression (month 17)

Progress: This subtask was accomplished in year 2. However, the rate of tumor take and growth of human prostate carcinoma MDA-PCa-2b was lower than expected (as reported in year 2 progress report). This subtask was repeated using different cell numbers. However, while the percent of mice that developed tumors increased, the length of time required for the tumor growth hindered experimental protocols. In addition, successful castration and development of castration resistant tumors was not improved. Consequently, tumors used within these studies were of various ages, sizes, and complexity. Thus our progress with in vivo studies has been hindered.

Subtask 3b: Optimize live ^{18}F -choline PET/CT imaging of nude mice bearing MDA-PCa-2b human prostate carcinoma xenograft model at 15 weeks post-castration (month 21)

Progress: This subtask was accomplished in year 2. We were unable to acquire or synthesize ^{18}F -choline in enough purity for these studies in year 3, thus, we attempted to utilize 18-FDG for imaging of MDA-PCa-2b human prostate carcinoma tumors. Unfortunately, the tumor uptake of 18-FDG by MDA-PCa-2b tumors was minimal.

We first verified the 18-FDG uptake within MDA-PCa-2b cells. After a 2 hour room temperature incubation of MDA-Pca-2b cells with 18-FDG about 1/3 of the activity was retained within the cells (data not shown). We next incubated molecularly targeted anti-TF p30-1 peptide/Qdot complex with the same MDA-PCa-2b cells, followed by Cerenkov and CRET imaging. It became apparent that the CRET signal was increasing the Cerenkov luminescent signal. This can be observed in Figure 20b when comparing the Cerenkov luminescent signal between wells containing 10 nM and 1 nM p30-1/Qdot. To further investigate

this spectral overlap we repeated the experiment with 100 μCi 18-FDG per well, resulting in $\sim 38 \mu\text{Ci}$ internalized 18-FDG (Figure 21). To this we added a serial dilution of p30-1/Qdot. The resulting increase of Cerenkov luminescent signal ranges from $\sim 10\%$ up to $\sim 77\%$ and is listed in Table 3.

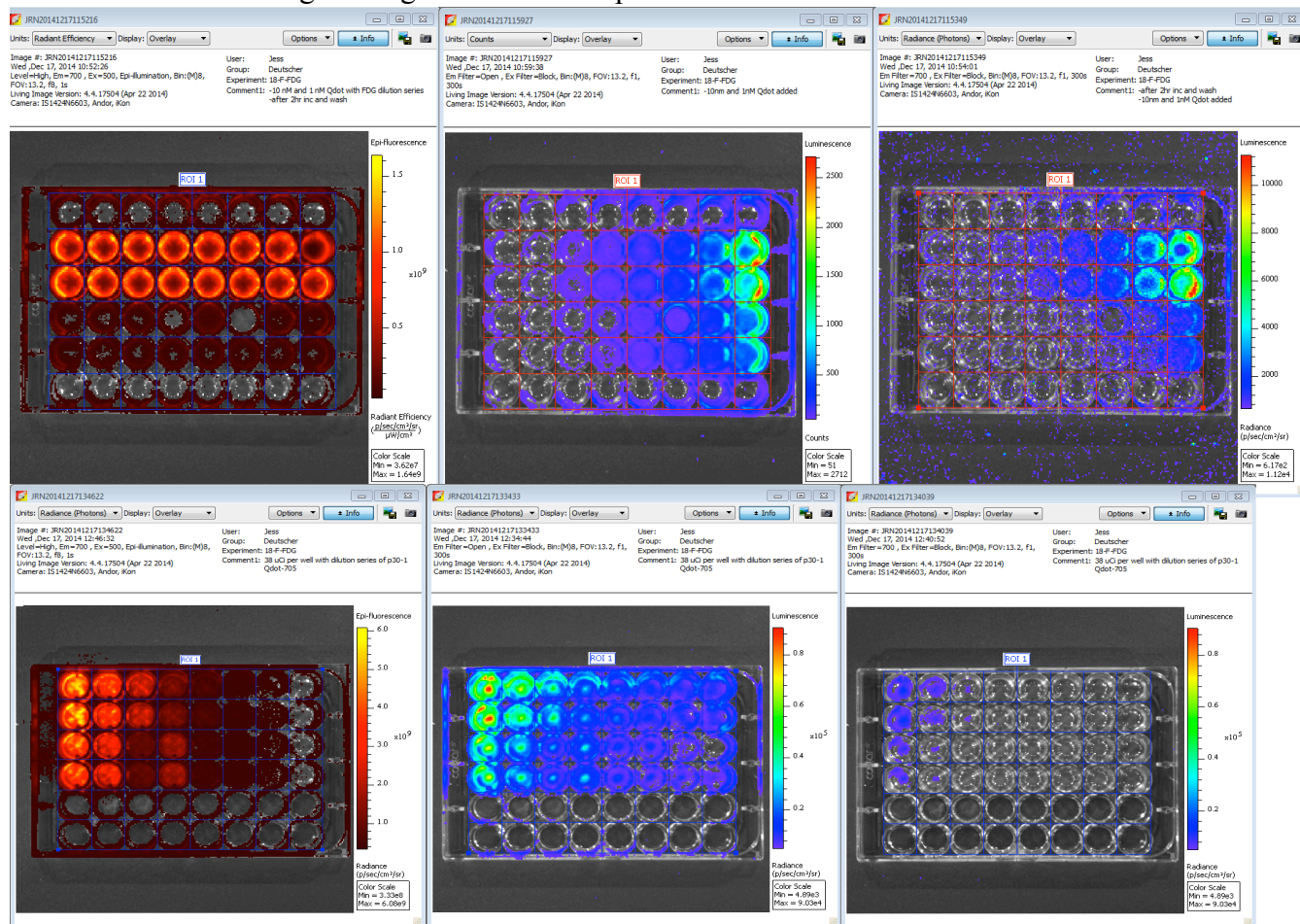


Figure 20. Optical Imaging of CRET Signal from Molecularly Targeted Qdot-705 and Internalized ^{18}F FDG within MDA-PCa-2b Human Prostate Carcinoma Cells. (A) Fluorescent imaging of 10 nM and 1 nM Qdot-705 complexed with p30-1 peptide bound to MDA-PCa-2b cells. (B) Open filter set for the imaging of Cerenkov emission from internalized ^{18}F FDG serial dilution. (C) CRET signal from 10 nM and 1 nM Qdot samples with internalized ^{18}F FDG. In short, MDA-PCa-2b cells were grown in 48 well plates and serum starved for 24 hours prior to the experiment. FDG dilution series containing 250, 125, 62.5, 31.3, 15, 7.5, 3.75, or 1.8 μCi was incubated with cells for 2 hours at room temperature, washed and subsequently incubated with 10 or 1 nM p30-1 peptide/Qdot complex for 30 minutes at room temperature. Cells were again washed and imaged as described.

Figure 21. Optical Imaging of CRET Signal from Molecularly Targeted Qdot-705 and Internalized ^{18}F FDG within MDA-PCa-2b Human Prostate Carcinoma Cells. (A) Qdot-705 serial dilution, (B) Cerenkov signal from internalized 38 μCi per well ^{18}F FDG, (C) resulting CRET dilution series were all imaged using an IVIS Spectrum. (D) Graph containing the quantification of each type

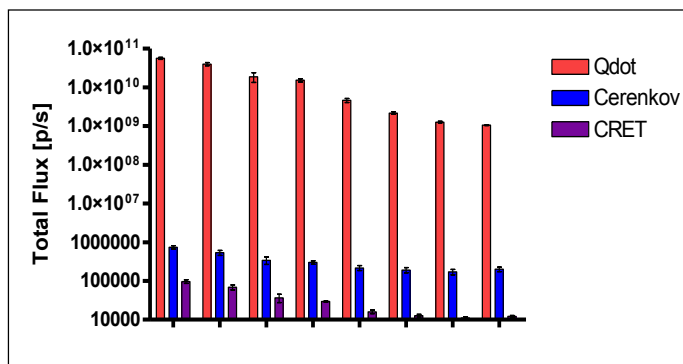


Table 3. Optical Output of Cerenkov Radiation, Qdot Fluorescence, and CRET.

Qdot Average Signal	StdDev	Cerenkov Average Signal	StdDev	% Increase of Cerenkov Signal	CRET Average Signal	StdDev	Ratio CRET:Qdot	Ratio CRET: Cerenkov
5.62E+10	6.41E+09	7.43E+05	1.51E+05	76.99	9.66E+04	2.11E+04	1.72E-06	1.30E-01
3.99E+10	7.34E+09	5.35E+05	1.63E+05	68.06	6.85E+04	1.93E+04	1.71E-06	1.28E-01
1.87E+10	1.06E+10	3.42E+05	1.47E+05	49.97	3.64E+04	1.80E+04	1.94E-06	1.06E-01
1.53E+10	2.84E+09	3.01E+05	6.17E+04	43.23	2.93E+04	2.33E+03	1.92E-06	9.73E-02
4.63E+09	1.14E+09	2.16E+05	6.36E+04	20.94	1.60E+04	3.24E+03	3.45E-06	7.39E-02
2.17E+09	3.24E+08	1.91E+05	5.86E+04	10.46	1.26E+04	2.06E+03	5.81E-06	6.61E-02
1.27E+09	1.19E+08	1.71E+05	5.58E+04	0	1.11E+04	1.47E+03	8.76E-06	6.48E-02
1.06E+09	4.71E+07	2.01E+05	5.28E+04	14.71	1.21E+04	1.53E+03	1.14E-05	6.04E-02

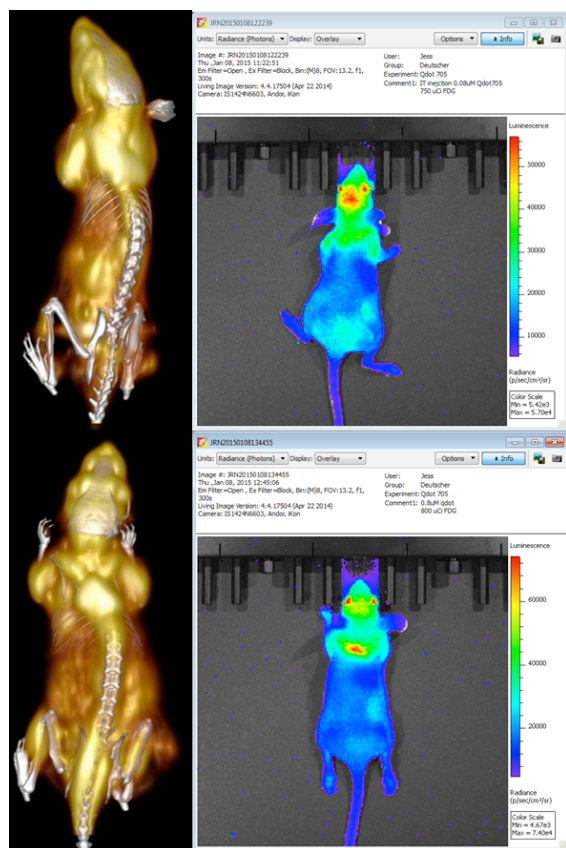


Figure 22. PET/CT and Cerenkov Imaging of 18-FDG within nude Mice Bearing Xenografted MDA-PCa-2b Human Prostate Carcinoma Tumors. Two castrated nude mice bearing castration resistant MDA-PCa-2b human prostate tumors were fasted overnight. These animals then received an I.P. injection of 800 μ Ci 18-FDG. The animals were then imaged 45 minutes post-injection.

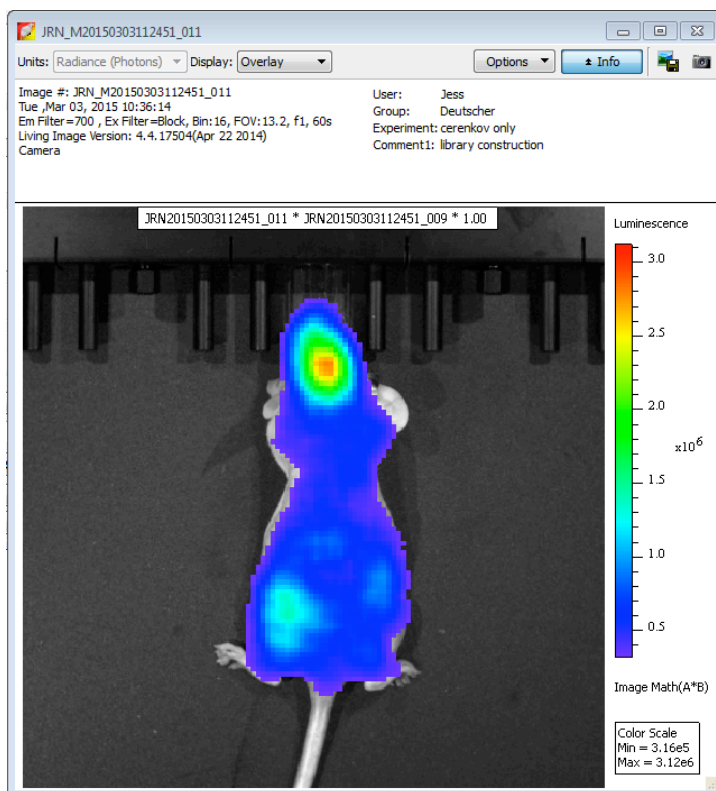


Figure 23. Cerenkov Imaging of 18-FDG within a nude Mouse. A fasted nude mouse was placed in a warm and dark environment for 30 minutes prior to receiving an I.P. injection of 300 μ Ci of 18-FDG. The mouse kept in the warm and dark environment for another 45 minutes, followed by Cerenkov imaging on a pre-warmed stage within the IVIS Spectrum.

Next, in vivo PET/CT and Cerenkov imaging of 18-FDG was performed in nude mice. The first attempt of 18-FDG imaging is represented in Figure 22. Two nude mice bearing castration resistant MDA-PCa-2b tumors

were given a high dosage of 18-FDG, unfortunately, even this high dosage of 18-FDG did not result in sufficient tumor uptake for either PET/CT or Cerenkov imaging of the tumors. Additional problems were

encountered with high brown fat uptake of the 18-FDG. The next attempt at 18-FDG imaging utilized a nude mouse with a regressed MDA-PCa-2b tumor (Figure 23). This mouse was kept within a warm and dark environment to prevent brown fat uptake. These studies will be verified with ^{18}F -choline.

Subtask 3c: Fluorescent optical imaging of molecularly targeted QDs in nude mice bearing MDA-PCa-2b human prostate carcinomas at 15 weeks post-castration.

Progress: This subtask was initiated within year 2 and completed in year 3. We inoculated nude mice with MDA-PCa-2b human prostate carcinoma cells. Data includes molecularly targeted imaging of p30-1/Qdot within a nude mouse bearing a castration resistant MDA-PCa-2b tumor (Figure 24).

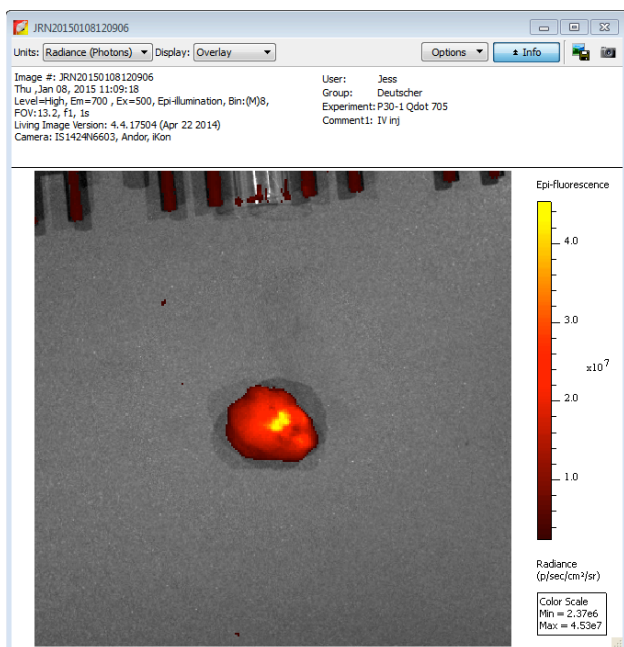


Figure 24. Optical Imaging of Molecularly Targeted p30-1/Qdot-705 within a nude Mouse Bearing a Xenografted MDA-PCa-2b Human Prostate Carcinoma Tumor. A castrated nude mouse bearing a castration resistant MDA-PCa-2b human prostate carcinoma tumor received an I.V. injection of 150 μL of 0.05 μM p30-1/Qdot705. The animal was then sacrificed 2 hours post-injection and the tumor harvested and fluorescently imaged using the IVIS Spectrum machine.

Tumor uptake of anti-TF, streptavidin coated QD with biotinylated p30-1 peptide, at 2 hours post-injection was imaged. However, the tumor to blood ratio was low. Thus further investigation, within year 3, of the pharmacokinetic profile of anti-TF, streptavidin coated QD with biotinylated p30-1 peptide, was performed in two non-castrated mice bearing MDA-PCa-2b tumors. The tumor uptake and retention of the molecularly targeted QD at 24 hours was not easily detectable within the images of the live mice (Figure 25). Ex vivo imaging of the excised tumors and organs revealed low tumor uptake and retention within only one of the tumors, which highlights the heterogeneity of this tumor model (Figure 26).

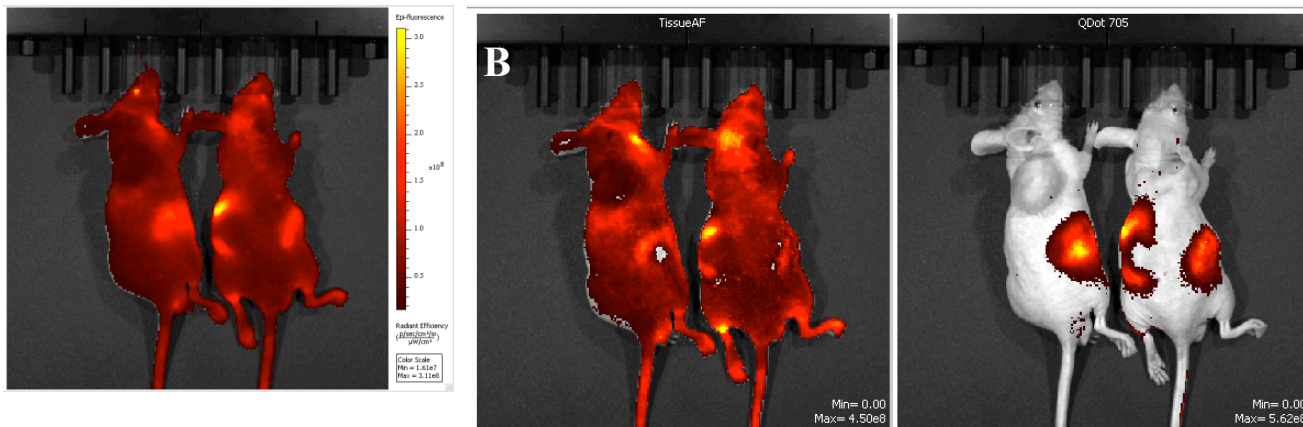


Figure 25. Optical Imaging of Molecularly Targeted p30-1/Qdot-705 within Intact Mice Bearing a Xenografted MDA-PCa-2b Human Prostate Carcinoma Tumors. Two non-castrated nude mice bearing MDA-PCa-2b human prostate carcinoma tumors received I.V. injections of 150 μL of 0.05 μM p30-1/SA-Qdot705. The animals were then (A) imaged 24 hours post-injection and (B) Living Image Software utilized to spectrally unmix the autofluorescence from the QD fluorescence.

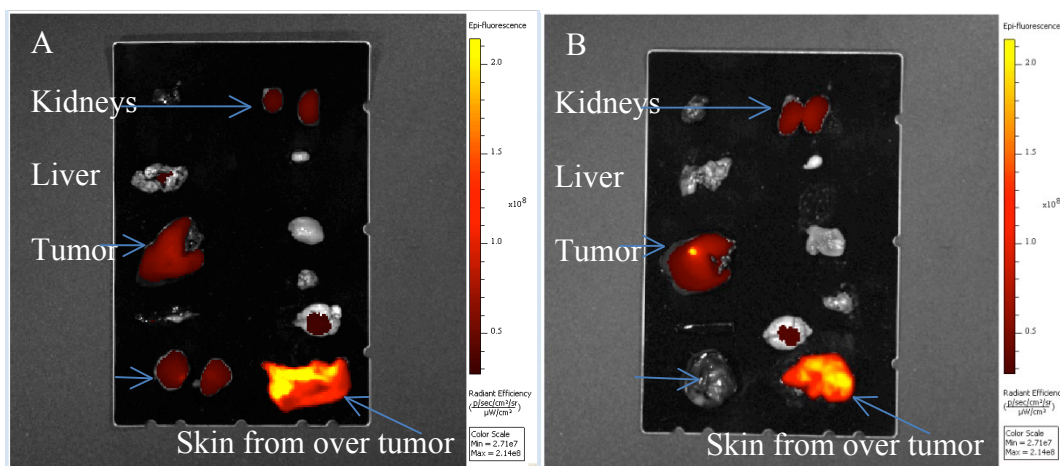


Figure 26. Ex Vivo Imaging of the Biodistribution of the Molecularly Targeted p30-1/SA-QD705 within Intact Mice Bearing a Xenografted MDA-PCa-2b Human Prostate Carcinoma Tumor. Two non-castrated nude mice bearing MDA-PCa-2b human prostate carcinoma tumors received I.V. injections of 150 μ L of 0.05 μ M p30-1/SA-Qdot705. The animals were then sacrificed and the tumors, organs, and tissues excised for ex vivo imaging.

It was hypothesized that the streptavidin coated QD could negatively affect the biodistribution of the p30-1/SA-QD705. One possible reason could be that the SA coated QD is much larger in diameter than the PEGylated QD, another possible explanation could be the surface charge of the SA proteins. Consequently, we purchased ITK Amino (PEG) QD (Invitrogen) for chemical coupling of peptides to QDs. These QDs are coated with amine-derivatized PEG. Consequently, we coupled the native carboxylic acid of the anti-TF and the anti-ErbB3 peptides to the amine-derivatized PEG using EDC. Unfortunately, this chemistry was not an option for the anti-ErbB2 peptide, KCCYSL, due the lysine within its sequence. Thus, this peptide was still used as a biotinylated peptide with an SA coated QD.

Subtask 3d: Pharmacokinetic analysis and comparative fluorescent imaging of molecularly targeted QDs in castrated and non-castrated nude mice bearing MDA-PCa-2b human prostate carcinoma xenografts.

Progress: Subcutaneous MDA-PCa-2b tumors were established in nude male mice. Of the mice inoculated, only 40% grew tumors at the expected rate. Once these tumors grew to 0.5 cm diameter one half of the mice were castrated. Following castration, as expected, the tumors regressed and regrew. These mice were then utilized for comparative optical imaging and further pharmacokinetic analysis of the new chemically coupled molecularly targeted QDs. Mice received tail vein injections of a mixed sample of QDs containing equal amounts of anti-ErbB3/QD605, anti-ErbB2/QD655, and anti-TF/QD705. Mice were then optically imaged, sacrificed, and the tumors and organs resected for ex vivo imaging and quantification of fluorescent signal (Figures 27 and 28).

Within the non-castrated mice, mouse #4 was utilized as a negative control. This mouse received QDs with no covalently attached molecularly targeting peptides. As expected there was no tumor uptake and only very low uptake within the clearance organs (Figure 27). Within the mice #1 through #3, which received molecularly targeted QDs, only mouse #3 had any tumor above background levels.

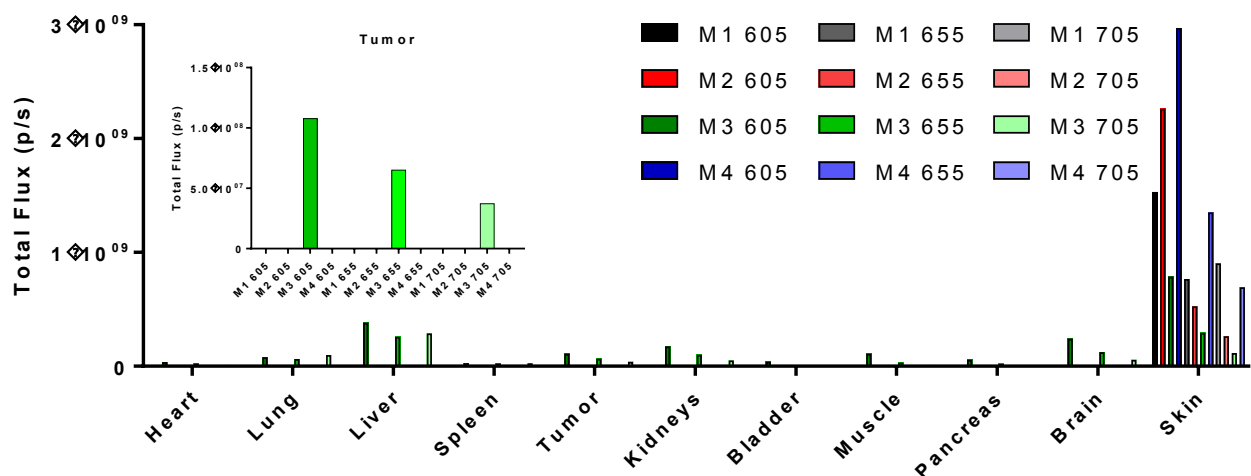


Figure 27. Ex Vivo Imaging of the Biodistribution of the Molecularly Targeted anti-ErbB3/QD605, anti-ErbB2/QD655, and anti-TF/QD705 within Non-Castrated Nude Mice Bearing MDA-PCa-2b Human Prostate Carcinoma Tumor Xenografts. Non-castrated mice bearing MDA-PCa-2b tumors #1 through #3 received tail vein injections of 100 μL of 0.5 μM mixed QD samples containing anti-ErbB3/QD605, anti-ErbB2/QD655, and anti-TF/QD705, while, mouse #4 received an equal mix of QDs with no molecular targeting peptides. The QDs were allowed to circulate for 24 hours before the mice were imaged, sacrificed, and organs and tissues resected for further imaging and quantification.

In comparison, the tumor uptake of the same mixed QD sample within castrated nude mice bearing MDA-PCa-2b hormone refractory tumors had significantly improved tumor uptake and retention of anti-ErbB3/QD605 (Figure 28). Anti-ErbB2/QD655 and anti-TF/QD705 tumor uptake and retention were also slightly improved when compared to the non-castrated tumor bearing mice. However, the lung and muscle uptake and retention was unexpected. Consequently, the tumor and select organs were collected, fixed in 10% buffered formalin, embedded in paraffin, and sliced for histological examination. After rehydration and epitope recovery the tumor tissues were blocked and probed for various biomarkers (Figures 29 and 30).

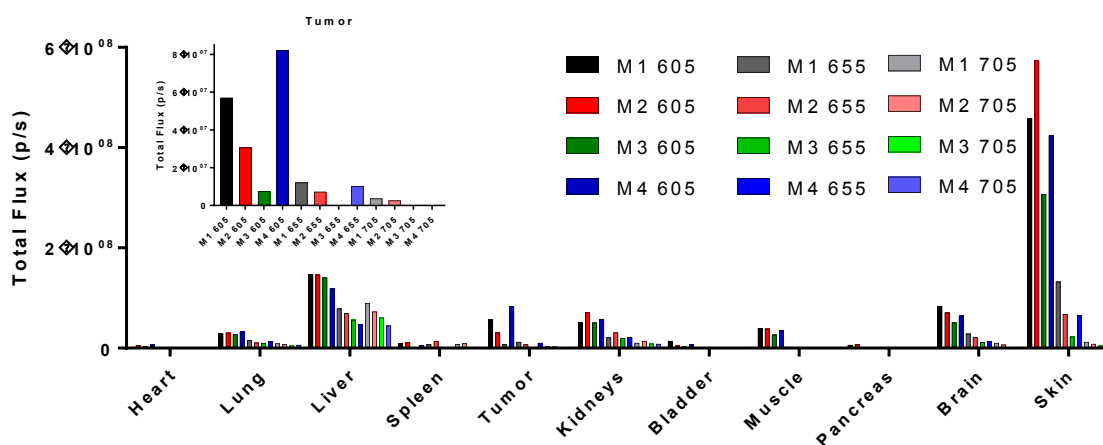


Figure 28. Ex Vivo Imaging of the Biodistribution of the Molecularly Targeted anti-ErbB3/QD605, anti-ErbB2/QD655, and anti-TF/QD705 within Castrated Nude Mice Bearing MDA-PCa-2b Human Prostate Carcinoma Tumor Xenografts. Castrated mice bearing MDA-PCa-2b tumors received tail vein injections of 100 μL of 0.5 μM mixed QD samples containing anti-ErbB3/QD605, anti-ErbB2/QD655, and anti-TF/QD705. The QDs were allowed to circulate for 24 hours before the mice were imaged, sacrificed, and organs and tissues resected for further imaging and quantification.

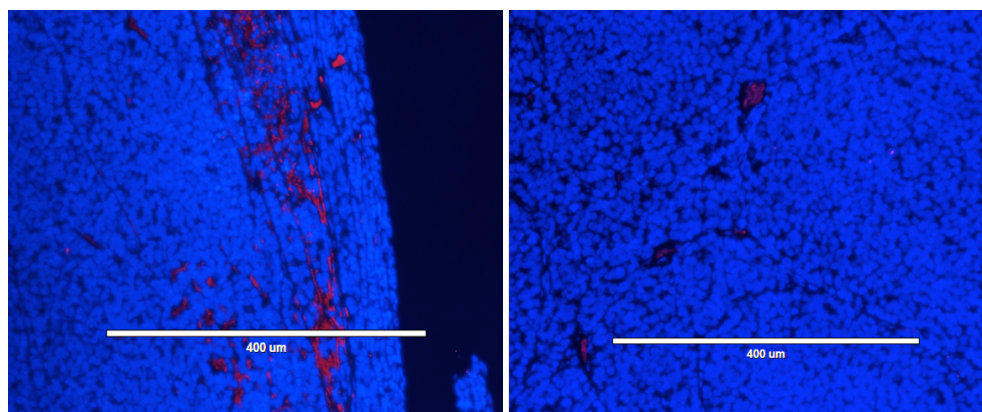


Figure 29. Microscopic Imaging of the Tissue Penetration of the Molecularly Targeted anti-ErbB3/QD605, anti-ErbB2/QD655, and anti-TF/QD705 within MDA-PCa-2b Human Prostate Carcinoma Tumor Xenografts. Castrated mice bearing MDA-PCa-2b tumors which received tail vein injections of mixed QD samples were sacrificed 24 hours post-injection and organs and tissues resected for further processing and analysis. Here, FFPE tumor tissue was de-paraffinized, re-hydrated, and submitted to epitope recovery prior to blocking and DAPI staining.

Initial histological investigation into the tumor uptake and retention of the QDs was performed using 5 micron thick slices of tumor tissue which was counter stained with DAPI to identify the nuclei of cells and help delineate areas of tissue from vasculature and interstitial spaces. Figure 29 shows the vast majority of the QDs are contained within the vasculature and interstitial spaces with only 3 or 4 potential points of QD fluorescent signal within the actual tumor tissue. This data shows that the QDs are unable to extravasate the vasculature. This taken in combination with the lung and muscle uptake is suggestive of aggregation of the QDs.

Further exploration into the biomarkers revealed heterogeneity within each tumor type (ie. hormone sensitive versus hormone refractory). For example, the androgen receptor (AR) was expected to be present in hormone sensitive tumors from non-castrated mice and absent in hormone refractory tumors from castrated mice. However, the levels of AR found within non-castrated mice #2, #3 and #4 were surprisingly low in comparison to non-castrated mouse #1. Additionally, castrated mice #3 and #4 seemed to retain an unexpected amount of AR even after 15 weeks post-castration. Similar issues were found with ErbB3 levels and TF levels (PNA staining). Interestingly, heterogeneity was also found within individual tumors as well (data not shown). But importantly, over all, the hormone refractory tumors resected from the castrated mice possessed higher levels of the probed biomarkers. This data is in agreement with the ex vivo imaging analysis of the biodistribution of the molecularly targeted QDs (Figure 30).

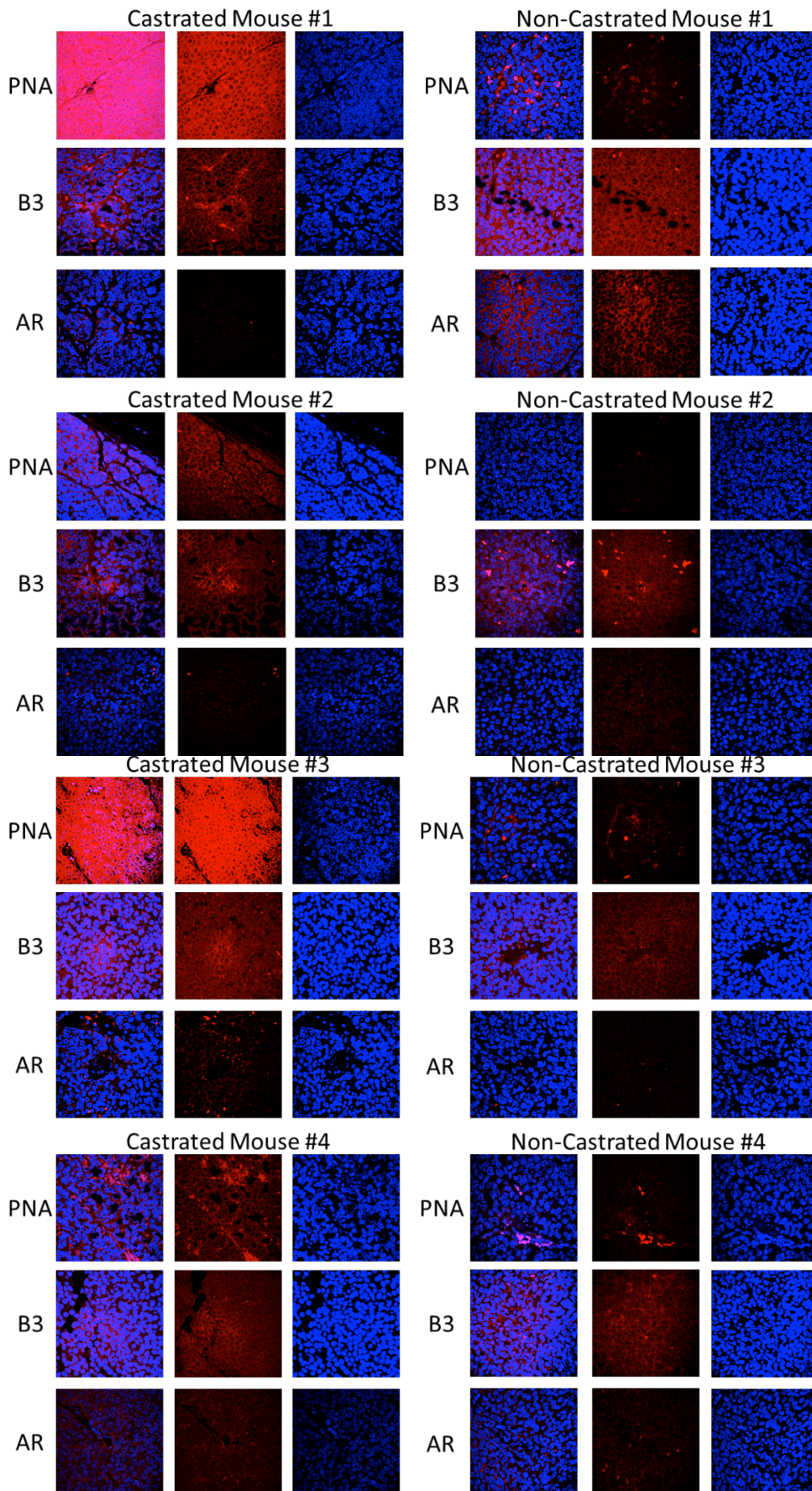


Figure 30. Microscopic Imaging of Biomarkers within Excised MDA-PCa-2b Tumors from Non-Castrated and Castrated Nude Mice. Castrated and non-castrated mice bearing MDA-PCa-2b tumors which received tail vein injections of mixed QD samples were sacrificed 24 hours post-injection and organs and tissues resected for further processing and analysis. Here, FFPE tumor tissue was de-paraffinized, re-hydrated, and submitted to epitope recovery prior to blocking, biomarker staining, and DAPI staining.

We took a few steps back and attempted to optimize the fluorescence output signal of the four Qdots used in the project, Qdot605, Qdot655, Qdot705, and Qdot805. As shown in Figure 31, the output for mixed QDots was readily visible with 465nm excitation and 660nm and 700nm emission (B and C). However, little emission occurred in the others.

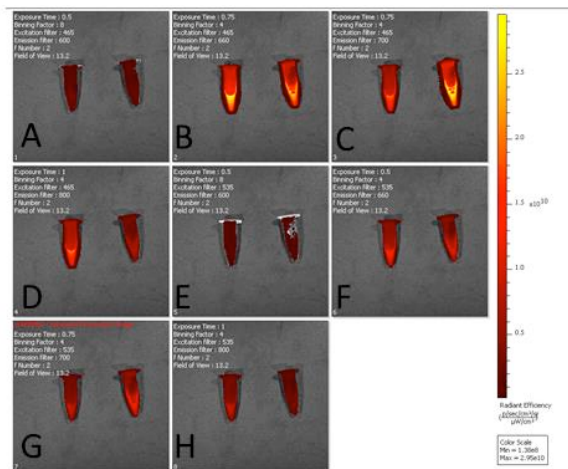


Figure 31. Qdot Fluorescence Output. The four types of Qdots utilized for this project, Qdot605, Qdot655, Qdot705, and Qdot805, were mixed together in equal amounts and imaged using two different excitation/emission filter sets for direct comparison. Within each image are two tubes, one containing 1x Qdot mixture and the other 0.5x Qdot mixture. Images A – D were each acquired using an excitation filter of 465nm. The emission filters utilized were 600nm, 660nm, 700nm, and 800nm, respectively. Images E – H were acquired using excitation filter of 535nm, while the emission filters were 600nm, 660nm, 700nm, and 800nm, respectively.

Because the peptides may not have the appropriate in vivo properties for imaging, biodistribution was analyzed with an additional peptide in the mixture that binds prostate cancers (CD44v6 targeting peptide) in an attempt to get imaging signal in the tumors. Four MDA-PCa-2b mice were analyzed but little if any tumor uptake was found. A representative ex vivo image analysis is shown in Figure 32.

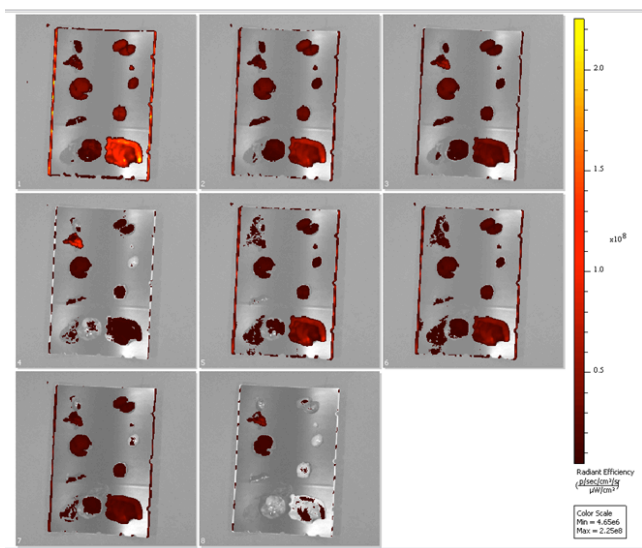


Figure 32. Biodistribution of Molecularly Targeted Qdots within Castrated Nude Mice Bearing MDA-PCa-2b Human Prostate Carcinoma Tumor Xenografts. Anti-ErbB3/QD605, anti-ErbB2/QD655, anti-TF/QD705, and anti-CD44v6/QD805 were mixed at an equimolar concentration of 0.5 uM. 100 ul of the QD mixture was intravenously injected and allowed to circulate for 24 hours before the mice were imaged, sacrificed, and organs and tissues resected for further imaging and quantification.

Key:	Heart	Kidneys
	Lung	Bladder
	Liver	Muscle
	Spleen	Pancreas
	Tumor	Brain
		Skin from over tumor

Task 4. Standardize Protocol for In Vivo Multiplexed CRET Imaging of Nude Mice (Castrated and Intact) Bearing MDA-PCa-2b Human Prostate Carcinoma Xenografts.

Subtask 4a: Inoculation and castration of 9 nude mice to generate the MDA-PCa-2b human xenograft model of prostate carcinoma progression (month 24)

Progress: We inoculated nude mice with MDA-PCa-2b human prostate carcinoma cells and analyzed CRET imaging in years 2 and 3. Data is presented below.

Subtask 4b: Standardize CRET multiplexed optical imaging in nude mice (intact, 1 week post-castration, and 15 weeks post-castration) bearing MDA-PCa-2b human prostate carcinoma xenografts (months 28-29)

Progress: The first attempt at in vivo CRET imaging was performed within a nude mouse with no tumor (data not shown).

Additional in vivo CRET imaging was performed within three nude mice with MDA-PCa-2b tumors (Figure 33). The mice were fasted overnight and placed in a warm and dark environment to prevent brown fat uptake. Each mouse then received an I.P. injection of 18-FDG followed immediately by intra-tumoral injection of molecularly targeted p30-1/Qdot. Tumor 1 received 0.8 μM , Tumor 2 received 0.08 μM , and Tumor 3 received 0.008 μM intra-tumoral injection. After 30 minutes the mice were sacrificed and tumors harvested. Fluorescent imaging revealed that the molecularly targeted p30-1/Qdot was still localized within the tumor. However, each tumor had varying levels of 18-FDG uptake and retention 1, 1.3, and 0.7 μCi , were measured in Tumors 1, 2, and 3, respectively.

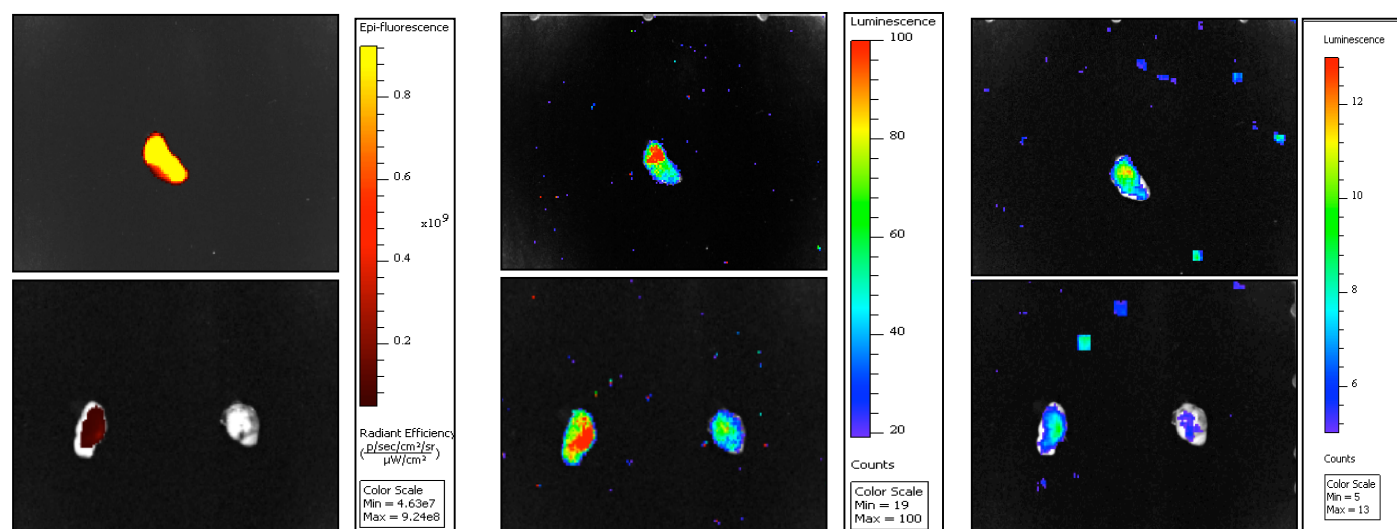


Figure 33. Optical Imaging of p30-1/Qdot-705 CRET Signal within MDA-PCa-2b Tumors. Three fasted nude mice were placed in a warm and dark environment for 30 minutes prior to receiving an I.P. injection of 300 μCi of 18-FDG followed immediately by intra-tumoral injections of, 0.8 μM , 0.08 μM , or 0.008 μM p30-1/Qdot. The mice were kept in the warm and dark environment for another 30 minutes, followed sacrifice, tumor harvest, and optical imaging: fluorescent imaging (A), luminescent Cerenkov imaging (B) and CRET imaging (C).

Task 5. Evaluate Diagnostic/Staging Potential of Multiplexed CRET Imaging within TRAMP Mice.
Evaluate Diagnostic/Staging Potential of Multiplexed CRET Imaging within TRAMP Mice (months 30-36).

Progress. First we determined expression levels of the desired targets in cultured TRAMP-C2 cell lines. We examined the levels of gal-3 in cultured TRAMP-C2 and human prostate cancer cell lines. As shown in Figure 34, TRAMP-C2 mouse and human DU-145 prostate cancer cells express high levels of gal-

3. For TF antigen, the P30-1 peptide bound both to TRAMP-C2 and PC3 cells (Figure 35). Thus, we were initially going to focus on peptides that bind these antigens.

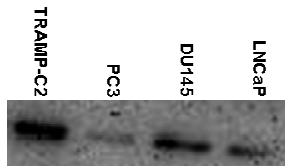


Figure 34. Gal-3 Protein Levels in Prostate Carcinoma Cell Lines. Assessment of total gal-3 protein within four different prostate carcinoma cell lines was performed via immunoblot analysis with a gal-3 monoclonal antibody.

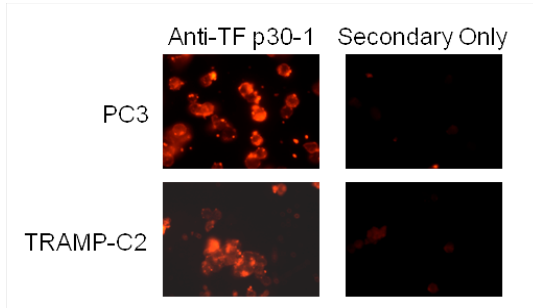


Figure 35. Confocal Microscopy Analysis of Binding of TF-avid Peptide to TRAMP-C2 Cells. Binding of biotinylated p30-1 to mouse TRAMP-C2 and human PC3 prostate carcinoma cells.

Subtask 5a: TRAMP mice (ages 8, 12, 16, or 20 weeks old) with and without castrations will be imaged utilizing the standardized multiplexed CRET imaging protocol (30 mice) (months 31 – 36).

Progress: We had a difficult time getting in vivo CRET imaging to work due to sensitivity issues. We attempted to establish enough TRAMP mice to perform the in vivo imaging (no-cost extension) and continued to explore CRET imaging potential in castrated and non-castrated MDA-PCa-2b human prostate carcinoma xenografts. However, a colony of TRAMP mice was not successfully generated at the In Vivo Imaging Core.

Subtask 5b: Histopathologic analysis of imaged TRAMP mice to validate diagnosis of stage of tumor development and/or progression (months 31-36).

Progress: We wanted to compare histology of imaged mice to TRAMP mice with progression of prostate cancer (Figure 36). We were not able to complete this task in this time frame.

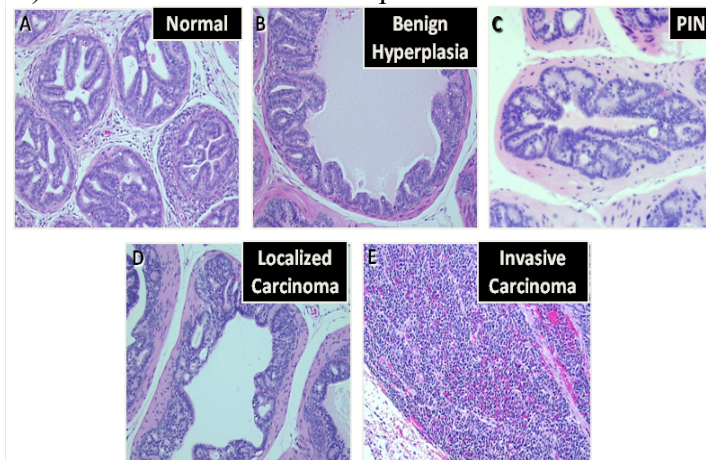


Figure 36. Stages of prostate carcinoma development in the TRAMP mouse model. Fixed and paraffin embedded prostate tissues from TRAMP mice received standard H&E staining for histopathologic analysis. (A) Normal prostate tissue of the TRAMP mouse. (B) Benign hyperplasia of the TRAMP mouse develops, on average, at the age of 8 weeks of age and (B) progresses to PIN by approximately 12 weeks of age. (C) Localized carcinoma will be apparent in most TRAMP mice between the ages of 16 to 18 weeks old (D) and will develop into invasive carcinoma by 20 weeks.

Key Research Accomplishments

- Purify large quantities of ErbB2 ECD.
- Perform stability studies in vitro of ErbB2 and ErbB3, and heterodimer.
- Optimize ELISA for ErbB2/ErbB3 dimerization.
- Perform ELISA showing ErbB2 and ErbB3 react with anti- ErbB2 and ErbB3 antibodies and ErbB2/ErbB3 can be captured in microtiter plate well and heregulin promotes ErbB2/ErbB3 heterodimer.
- Perform in vitro phage display selections with ErbB2, ErbB3, ErbB2/ErbB3, and heregulin treated ErbB2/ErbB3.
- Perform in vivo phage selections in MDA-PCa-2b human prostate cancer cell xenografted male mice.
- Developed and optimized protocol for high throughput Next Gen sequencing. Identification and analysis of selected peptide sequences using Next Generation sequencing. Discovered sequence homology/motifs between the different selected phage populations.
- Sequence outputs of multiple in vitro and in vivo selections. Develop protocol for high throughput Next Gen sequencing.
- Analyze DNA sequencing data and displayed peptide sequences.
- Synthesize the TF, ErbB2 and ErbB3 avid peptides with a biotin for coupling to streptavidin coated QDs.
- Coupled TF, ErbB2 and ErbB3 avid peptides via biotin to streptavidin coated QDs.
- Characterize binding of TF, ErbB2 and ErbB3 avid QDs to human prostate MDA-PCa-2b carcinoma cells using flow cytometry, confocal microscopy and fluorescent imaging.
- Optimized imaging of components of CRET in tumor-bearing mice.
- Optically imaged p30-1/Qdot-705 CRET signal within MDA-PCa-2b Tumors.
- Synthesize the TF, ErbB2 and ErbB3 avid peptides with no biotin for chemical coupling to amine derivatized PEG coated QDs.
- Characterize binding of TF, ErbB2 and ErbB3 avid PEG-QDs to human prostate MDA-PCa-2b carcinoma cells using fluorescent imaging.
- Compare biodistribution of molecularly targeted SA-QD versus PEG-QD.
- Compare biodistribution of molecularly targeted QDs within hormone sensitive and hormone refractory MDA-PCa-2b tumor bearing mice.
- Microscopically analyze QD tumor penetration and biomarker expression of the MDA-PCa-2b tumors.

Reportable Outcomes

- Invited Speaker “Phage Display for Tumor Imaging Agents” University of Missouri Research Reactor, November 2013.
- Newton-Northup JR, Dickerson MT, Deutscher SL. (2015, April) Phage Display Selection of ErbB2/ErbB3 Targeting Peptides. Poster session presented at the University of Missouri Life Sciences Week Columbia, MO.

Conclusions

In summary, we have shown that biomarker status is indeed changed, as predicted, within hormone refractory MDA-PCa-2b tumors as compared to hormone sensitive MDA-PCa-2b tumors. However, the cancer biology/ biochemistry are more complex and heterogeneous than originally hypothesized. This finding resulted in possible QD aggregation, lack of QD extravasation/tissue penetration, and unpredictable tumor take and tumor growth rates. The anti-TF and anti-ErbB3 QD could be visualized in MDA-PCa2b human prostate cancer xenografts using an ex vivo-in vivo CRET imaging protocol. The anti-TF QD gave

the most positive results. We tried to optimize tumor take and uptake rates and improve peptides for better optimization and utility in vivo. QDots were too big to provide excellent pharmacokinetics in vivo however. In the no cost extension period, we had also hoped to study the CRET imaging capabilities in TRAMP mice. Imaging was not achieved, as establishing and maintaining TRAMP mice for optical imaging in vivo was not successful.

We have shown that we can form ErbB2/ErbB3 heterodimers in vitro and we can promote heterodimer formation in human prostate cancer MDA-PCa-2b cells. Phage display selections against ErbB2/ErbB3 complexes resulted in numerous peptide sequences of interest. Two peptides (B2/B3#3 and #9) bound with highest affinity (1.71 μ M and 1.08 μ M, respectively) and specificity to ErbB2/ErbB3. Furthermore, the phage display selected peptides and the TF-binding peptide, p30-1, bound to prostate cancer cells expressing high levels appropriate antigens. Additionally, imaging of each independent component of the CRET system was optimized and a CRET imaging protocol was developed. The anti-TF QD could be visualized in MDA-PCa-2b human prostate cancer xenografts using an ex vivo-in vivo imaging protocol. However, imaging with a mixture of QD coupled peptides did not generate decipherable images probably due to lack of sensitivity and overlap in excitation and emissions for in vivo/ex vivo imaging due to unforeseen complexities of the biological microenvironment of the animal.

So What?

- We have shown that we can form ErbB2/ErbB3 heterodimers in vitro and we can promote heterodimer formation in human prostate cancer MDA-PCa-2b cells.
- CRET imaging has been developed and used with marginal success in molecular imaging.
- The TF-targeting peptide-QD could be used to visualize MDA-PCa-2b cells.

References:

1. Timothy L. Bailey and Charles Elkan, "Fitting a mixture model by expectation maximization to discover motifs in biopolymers", *Proceedings of the Second International Conference on Intelligent Systems for Molecular Biology*, pp. 28-36, AAAI Press, Menlo Park, California, 1994.

Bibliography:

- Invited Speaker "Phage Display for Tumor Imaging Agents" University of Missouri Research Reactor, November 2013.
- Newton-Northup JR, Dickerson MT, Deutscher SL. (2015, April) Phage Display Selection of ErbB2/ErbB3 Targeting Peptides. Poster session presented at the University of Missouri Life Sciences Week Columbia, MO.

Personnel:

Deutscher, Susan L
Dickerson, Marie Terese Kremer
Dye, Chandler Michael
Newton Northup, Jessica Rose
Nicholl, Michael B
Quinn, Jeanne Marie
Quinn, Thomas P
Soendergaard, Mette

Appendices: Poster Abstract and Animal Usage

Abstract

The EGFR family of receptors propels numerous carcinomas including those on breast, ovary, and prostate via homo- and hetero-dimerization with other EGFR family receptors. Of the four known EGFR family members ErbB2 has received the most attention in terms of viable tumor targets. ErbB2 heterodimerizes with other family members, most notably ErbB3. ErbB3 upon activation with neuregulin (NRG) will heterodimerize with ErbB2 activating several signaling pathways resulting in increased tumor growth and decreased apoptosis. ErbB-3 has now been linked to progression of cancer and resistance to several therapies. ErbB3, usually present at low to moderate receptor numbers, can be upregulated through inhibition of other ErbB family members and certain cellular stresses, including chemotherapeutics. Even though it has become clear that the heterodimer, ErbB2/ErbB3 (B2/B3), plays a critical role in signaling and cancer, currently there is no available clinical assay for assessment of B2/B3 status. The ability to detect B2/B3 status could provide diagnosis of high risk carcinomas. To this end, we hypothesized that bacteriophage (phage) display could be exploited to select for peptide sequences specific for B2/B3 heterodimer. Phage display selection was employed against purified extracellular domain (ECD) of B2/B3 -ECD heterodimer. Next generation sequencing revealed a six amino acid motif for B2/B3 heterodimer targeting. This B2/B3 targeting motif was generated from 13 unique sequences of which four have been validated as able to bind heterodimer. Future work will include in vitro and in vivo characterization of the selected anti-ErbB2/B3 peptides.

Animal approval/use/pain category:

Initial approval VA IACUC ACORP 139 approved 2/11/2013 = MU IACUC #7750 3/6/2013 =ACURO approved 4/8/2013 = 18 total animals used Species: Mouse; Strain: Athymic nudes; Pain Category D

Triennial Rewrite VA IACUC ACORP 180 approved 1/29/2016 = MU IACUC #8671 2/8/2016 =ACURO approved 3/10/2016 = 30 total animals used Species: Mouse; Strain: Athymic nudes; Pain Category D